

Neural Operators for Bypassing Gain and Control Computations in PDE Backstepping

Luke Bhan, Yuanyuan Shi, and Miroslav Krstic

Abstract— We introduce a framework for eliminating the computation of controller gain functions in PDE control. We learn the nonlinear operator from the plant parameters to the control gains with a (deep) neural network. We provide closed-loop stability guarantees (global exponential) under an NN-approximation of the feedback gains. While, in the existing PDE backstepping, finding the gain kernel requires (one offline) solution to an integral equation, the neural operator (NO) approach we propose learns the mapping from the functional coefficients of the plant PDE to the kernel function by employing a sufficiently high number of offline numerical solutions to the kernel integral equation, for a large enough number of the PDE model’s different functional coefficients. We prove the existence of a Deep-ONet approximation, with arbitrarily high accuracy, of the exact nonlinear continuous operator mapping PDE coefficient functions into gain functions. Once proven to exist, learning of the NO is standard, completed “once and for all” (never online) and the kernel integral equation doesn’t need to be solved ever again, for any new functional coefficient not exceeding the magnitude of the functional coefficients used for training. We also present an extension from approximating the gain kernel operator to approximating the full feedback law mapping, from plant parameter functions and state measurement functions to the control input, with semiglobal practical stability guarantees. Simulation illustrations are provided and code is available on github. This framework, eliminating real-time recomputation of gains, has the potential to be game changing for adaptive control of PDEs and gain scheduling control of nonlinear PDEs.

The paper requires no prior background in machine learning or neural networks.

I. INTRODUCTION

ML/AI is often (not entirely unjustifiably) thought of as an ‘existential threat’ to model-based sciences, from physics to conventional control theory. In recent years, a framework has emerged [47], [48], [51], [52], initiated by George Karniadakis, his coauthors, and teams led by Anima Anandkumar and Andrew Stuart, which promises to unite the goals of physics and learning, rather than presenting learning as an alternative or substitute to first-principles physics. In this framework, often referred to as neural operators (NO), which is formulated as learning of mappings from function spaces into function spaces, and is particularly suitable for PDEs, solution/“flow” maps can be learned after a sufficiently large number of simulations for different initial conditions. (In some cases, parameters of models can also be identified from experiments.)

a) *Mappings of plant parameters to control gains and learning of those maps:* One can’t but ask what the neural operator reasoning can offer to control theory, namely, to the design of

The authors are with the University of California, San Diego, USA, luhan@ucsd.edu, yyshi@eng.ucsd.edu, krstic@ucsd.edu

controllers, observers, and online parameter estimators. This paper is the first venture in this direction, a breakthrough with further possibilities, and a blueprint (of a long series of steps) to learn PDE control designs and prove their stability.

In control systems (feedback controllers, observers, identifiers), various kinds of nonlinear maps arise, some from vector into vector spaces, others from vector or function spaces into function spaces. Some of the maps have time as an argument (making the domain infinite) and others are mappings from compact domains into compact image sets, such as mappings converting system coefficients into controller coefficients, such as the mapping $K(A, B)$ for the closed-loop system $\dot{x} = Ax + Bu$, $u = Kx$ (under either pole placement or LQR).

While learning nonlinear maps for various design problems for nonlinear ODEs would be worth a study, we focus in this initial work one step beyond, on a benchmark PDE control class. Our focus on an uncomplicated—but unstable—PDE control class is for pedagogical reasons. Combining the operator learning with *PDE backstepping* is complex enough even for the simplest-looking among PDE stabilization problems.

b) *PDE backstepping control with the gain computation obviated using neural operators:* Consider 1D hyperbolic partial integro-differential equation systems of the general form $v_t(x, t) = v_x(x, t) + \lambda(x)v(x, t) + g(x)v(0, t) + \int_0^x f(x, y)v(y, t)dy$ on the unit interval $x \in [0, 1]$, which are transformable, using an invertible backstepping “pre-transformation” introduced in [6] into the simple PDE

$$u_t(x, t) = u_x(x, t) + \beta(x)u(0, t) \quad (1)$$

$$u(1, t) = U(t). \quad (2)$$

Our goal is the design of a PDE backstepping boundary control

$$U(t) = \int_0^1 k(1-y)u(y, t)dy. \quad (3)$$

Physically, (1) is a “transport process (from $x = 1$ towards $x = 0$) with recirculation” of the outlet variable $u(0, t)$. Recirculation causes instability when the coefficient $\beta(x)$ is positive and large. This instability is prevented by the backstepping boundary feedback (3) with the gain function $k(\cdot)$ as a kernel in the spatial integration of the measured state $u(y, t)$. (The full state does not need to be measured, as explained in Remark 1 at the end of Section IV.)

Backstepping produces the gain kernel k for a given β . The mapping $\mathcal{K} : \beta \mapsto k$ is nonlinear, continuous, and we learn it.

Why do we care to learn \mathcal{K} ? The kernel function k can always be computed for a particular β , so what is the interest in learning the *functional mapping/operator*? Once \mathcal{K} is learned, k no longer needs to be sought, for a new β , as a solution to a partial differential or integral equation. For the next/new

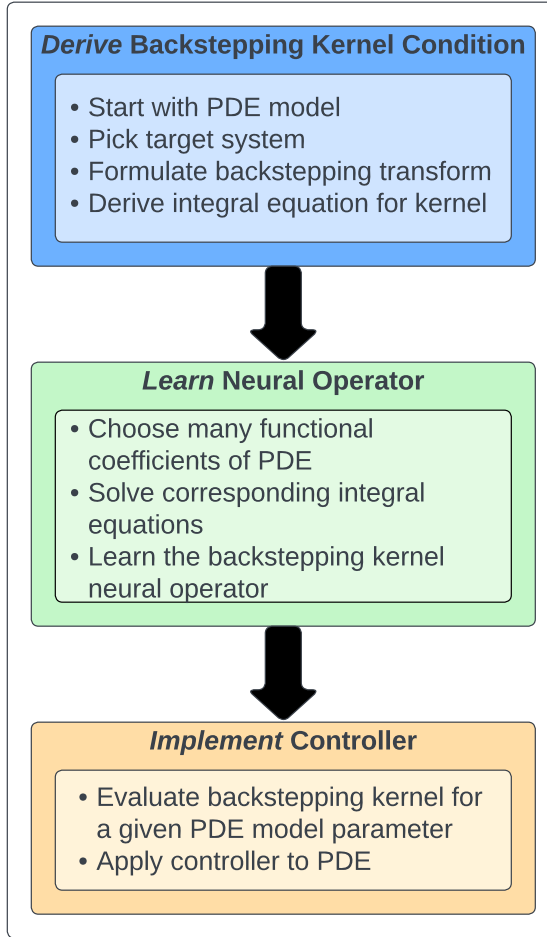


Fig. 1. An algorithmic representation of our design paradigm of employing neural operators in boundary control of PDEs. Three major step clusters are performed: (1) derivation of the integral equations for the backstepping kernels, performed only once; (2) learning of the mapping from the plant parameter functions into the backstepping kernel functions, also performed only once; and (3) implementation of the controller for specific plant parameters. The task in the top box has been completed in [40]. In this paper, the task in the middle box is introduced and stability guarantees for the task in the bottom box are provided.

β , finding k is simply a “function evaluation” of the learned mapping \mathcal{K} . This provides benefits in both adaptive control where, at each time step, the gain estimate \hat{k} has to be computed for a new parameter update $\hat{\beta}$, and in gain scheduling for nonlinear PDEs where the gain has to be recomputed at each current value of the state.

As well known, learning (ML, in general, and its operator learning varieties: DeepONet, FNO, LOCA, NOMAD, etc.) comes with an upfront price. Large data sets need to be first produced, and then large (possibly “deep”) neural networks need to be trained. There is no exception to this in the approach we propose. For a large sample set of recirculation functions β_i , we need to first solve for the corresponding backstepping kernels k_i . After that, a NN approximation of \mathcal{K} needs to be trained on that data set of the (β_i, k_i) pairs.

One can stop at producing the NN approximation of the

mapping \mathcal{K} and proceed with a heuristic use of the approximated gains \hat{k} . But we don’t stop there. We ask whether the PDE system will be still stabilized with the NN-approximated gain kernel \hat{k} . Our main theoretical result is affirmative. With a large enough data set of solved pairs (β_i, k_i) , and a large enough trained (deep) NN, closed-loop stability is guaranteed for a new β , not in the training set.

When ML is applied in the control context (as RL or other approaches), it is usually regarded as a model-free design. Our design, summarized in Figure 1, is not model-free; it is model-based. It is only that the computational portion of this model-based (PDE backstepping) design is obviated through ML.

Our learning is offline; not as in adaptive control [1], [6].

c) *Neural operator literature—a brief summary:* Neural operators are NN-parameterized maps for learning relationships between function spaces. They originally gained popularity due to their success in mapping PDE solutions while remaining discretization-invariant. Generally, nonlinear operators consist of three components: an encoder, an approximator, and a reconstructor [44]. The encoder is an interpolation from an infinite-dimensional function space to a finite-dimensional vector representation. The approximator aims to mimic the infinite map using a finite-dimensional representation of both the domain function space and the target function space. The reconstructor then transforms the approximation output into the infinite-dimensional target function space. The implementation of both the approximator and the reconstructor is generally coupled and can take many forms. For example, the original DeepONet [52] contains a “branch” net that represents the approximation network and a “trunk” net that builds a basis for the target function space. The outputs of the two networks are then taken in linear combination with each other to form the operator. FNO [48] utilizes the approximation network in a Fourier domain where the reconstruction is done on a basis of the trigonometric polynomials. LOCA [37] integrates the approximation network and reconstruction step with a unified attention mechanism. NOMAD [68] extends the linear reconstructor map in DeepONet to a nonlinear map that is capable of learning on nonlinear submanifolds in function spaces. There have been many more extensions to the neural operator architectures omitted here as they are usually designed around domain-specific enhancements [83] [49] [63]. Another line of work, called physics-informed neural networks (PINNs) [36], [66], which can be used as generic solvers of PDEs by adding physics constraint loss to neural networks. However, PINNs need to be re-trained for new recirculation function β , thus not providing as much acceleration for the computation of the backstepping kernels as the neural operators.

d) *Advances in learning-based control:* Among the first in demonstrating the stability of learning-based model predictive controllers (MPC) were the papers [2], [67], followed in several directions. First, for nonlinear systems, deep learning-based approaches consist of jointly learning the controller and(or) Lyapunov functions via NNs [10]–[14], [20], [21]. [10] proposed a method for learning control policies and NN Lyapunov functions using an empirical Lyapunov loss and then validating using formal verification. [11], [12] generalize the method to learning Lyapunov functions for piecewise linear

and hybrid systems, and [13] for learning regions of attraction of nonlinear systems. In addition, [59], [76] have explored how learning-based control will affect nominal systems with known Lyapunov functions, and [9], [22], [62] studied the problem of learning stability certificates and stable controllers directly from data. In a similar vein, [4] has developed a provable stable data-driven algorithm based on system measurements and prior knowledge for linear time-invariant systems.

In a separate, but related direction, many reinforcement learning (RL) [7], [74] control approaches have been developed over the past few years. On the one side, model-based RL has been studied due to its superior sample efficiency and interpretable guarantees. The main focus has been on learning the system dynamics and providing closed-loop guarantees in *finite-time* for both linear systems [15], [23], [29], [42], [77] (and references within), and nonlinear systems [5], [35], [43], [71]. For model-free RL methods, [30], [56], [60], [90] proved the convergence of policy optimization, a popular model-free RL method, to the optimal controller for linear time-invariant systems, [58], [61] for linear time-varying systems, [75] for partially observed linear systems. See [32] for a recent review of policy optimization methods for continuous control problems such as the LQR, H_∞ control, risk-sensitive control, LQG, and output feedback synthesis. For nonlinear systems, [16], [17], [19], [70] investigated policy optimization with stability guarantees in which the stability constraints are derived from control Lyapunov functions. In addition to policy optimization methods, [8], [46], [78], [79] have studied and proved the stability and asymptotic convergence of other model-free RL algorithms such as actor-critic methods [46], [79] and Q-learning [78] in control affine systems. In the domain of cyber-physical systems (CPS), a theoretical framework has been developed for learning-based control to handle partially observable systems [53].

Many advances have been made in learning-based control in games and multi-agent systems [31], [31], [50], [54], [55], [57], [64], [65], [80], [88], [89]. Convergence is characterized for various learning-based methods to Nash equilibria in zero-sum linear quadratic games [88], continuous games [55], Stackelberg games [31], [57], Markov games [54], [87], and multi-agent learning over networked systems [50], [64], [65]. A recent review for learning-based control in games is in [89].

We focus on learning-based control for PDE systems. In our previous work [69], we demonstrate the empirical success of using NOs for accelerating PDE backstepping observers, without theoretical guarantees. This work represents the first step towards using NOs for provably bypassing gain computations (with exponential stability guarantees) or directly learning the controller (with practical stability) in PDE backstepping.

e) Backstepping control of first-order hyperbolic PDEs: The PDE system (1), (2) is the simplest open-loop unstable PDE of any kind which can be of interest to the researcher working on PDE stabilization by boundary control. This system is treated here as a technical benchmark, as was done as well in [6] and a number of other references offering methodological advances in PDE stabilization. System (1), (2) is a particular case of a single-PDE hyperbolic class in [40] for which PDE backstepping was first introduced in the hyperbolic

setting. Coupled systems of first-order hyperbolic PDEs are of greater interest because they arise in fluid flows, traffic flows, elastic structures, and other applications. The first result on backstepping for a *pair* of coupled hyperbolic PDEs was in [18]. The extension from two to $n+1$ hyperbolic PDEs, with actuation of only one and with counterconvection of n other PDEs was introduced in [27]. An extension from $n+1$ to $n+m$ coupled PDEs, with actuation on m “homodirectional” PDEs, was provided in [33], [34]. Redesigns that are robust to delays were provided in [3]. An extension from coupled hyperbolic PDEs to cascades with ODEs was presented in [28]. An extension from hyperbolic PDE-ODE cascades to “sandwiched” ODE-PDE-ODE systems was presented in [81] and an event-triggered design for such systems was given in [82]. The extension of PDE backstepping to output-feedback regulation with disturbances is proposed in [25], [26]. For coupled hyperbolic PDEs with unknown parameters, a comprehensive collection of adaptive control designs was provided in the book [1]. Applications of backstepping to coupled hyperbolic PDE models of traffic are introduced in [84], [85].

f) Paper outline and contributions: After a brief introduction to the backstepping design in Section II, for system (1), (2), in Section III we prove that the backstepping kernel operator is locally Lipschitz, between the spaces of continuous functions, with which we satisfy a sufficient condition for the existence of a neural operator approximation of a nonlinear operator to arbitrarily high accuracy—stated at the section’s end in a formal result and illustrated with an example of approximating the operator $k = \mathcal{K}(\beta)$. In Section IV we present the first of our main results: the closed-loop stabilization (not merely practical but exponential) with a DeepONet-approximated backstepping gain kerne 1 function. In Section V we present simulation results that illustrate stabilization under DeepONet-approximated gains. Then, in Section VI we pose the question of whether we can not only approximate the gain kernel mapping $\beta(x) \mapsto k(x)$, as in Sections III and IV, but the entire feedback law mapping $(\beta(x), u(x, t)) \mapsto \int_0^1 k(1-y)u(y, t)dy$ at each time instant t ; we provide an affirmative answer and a guarantee of semiglobal practical exponential stability under such a DeepONet approximation. In Section VII we illustrate this feedback law approximation with a theory-confirming simulation. Then, in Section VIII, we present the paper’s most general result, which we leave for the end for pedagogical reasons, since it deals with Volterra operator kernel functions of two variables, (x, y) , on a triangular domain, and requires continuity of mappings between spaces of functions that are not just continuous but continuously differentiable, so that not only the backstepping kernel is accurately approximable but also the kernel’s spatial derivatives, as required for closed-loop stability. We close with a numerical illustration for this general case in Section IX.

In summary, the paper’s contributions are the PDE stabilization under DeepONet approximations of backstepping gain kernels (Theorems 2 and 4) and under the approximation of backstepping feedback laws (Theorem 3). Our stabilization results also hold for any other neural operators with a universal approximation property (shown for LOCA [37] and for FNO on the periodic domain [38]).

g) *Notation:* We denote convolution operations as

$$(a * b)(x) = \int_0^x a(x-y)b(y)dy \quad (4)$$

In the sequel, we suppresses the arguments x and t wherever clear from the context. For instance, we write (1), (2) compactly as $u_t = u_x + \beta u(0)$ and $u(1) = U$, where, from the context, the boundary values $u(0), u(1)$ depend on t as well.

II. BACKSTEPPING DESIGN FOR A TRANSPORT PDE WITH ‘RECIRCULATION’

Consider the PDE system (1), (2). We employ the following backstepping transformation:

$$w = u - k * u, \quad (5)$$

i.e., $w(x, t) = u(x, t) - \int_0^x k(x-y)u(y, t)dy$, to convert the plant into the target system

$$w_t = w_x \quad (6)$$

$$w(1) = 0 \quad (7)$$

with the help of feedback

$$U = (k * u)(1), \quad (8)$$

namely, $U(t) = \int_0^1 k(1-y)u(y, t)dy$. To yield the target system, k must satisfy the integral/convolution equation

$$k(x) = -\beta(x) + \int_0^x \beta(x-y)k(y)dy \quad (9)$$

for $x \in [0, 1]$. Note that, while this integral equation is linear in k for a given β , the mapping from β to k is actually nonlinear, due to the product in the convolution of β with k .

III. ACCURACY OF APPROXIMATION OF BACKSTEPPING KERNEL OPERATOR WITH DEEPONET

An n -layer NN $f^N : \mathbb{R}^{d_1} \rightarrow \mathbb{R}^{d_n}$ is given by

$$f^N(x, \theta) := (l_n \circ l_{n-1} \circ \dots \circ l_2 \circ l_1)(x, \theta) \quad (10)$$

where layers l_i start with $l_0 = x \in \mathbb{R}^{d_1}$ and continue as

$$l_{i+1}(l_i, \theta_{i+1}) := \sigma(W_{i+1}l_i + b_{i+1}), \quad i = 1, \dots, n-1 \quad (11)$$

σ is a nonlinear activation function, and weights $W_{i+1} \in \mathbb{R}^{d_{i+1} \times d_i}$ and biases $b_{i+1} \in \mathbb{R}^{d_{i+1}}$ are parameters to be learned, collected into $\theta_i \in \mathbb{R}^{d_{i+1}(d_{i+1})}$, and then into $\theta = [\theta_1^T, \dots, \theta_n^T]^T \in \mathbb{R}^{\sum_{i=1}^n d_{i+1}(d_{i+1})}$. Let $\vartheta^{(k)}, \theta^{(k)} \in \mathbb{R}^{\sum_{i=1}^k d_{k,(i+1)}(d_{k,i+1})}$ denote a sequence of NN weights.

An neural operator (NO) for approximating a nonlinear operator $\mathcal{G} : \mathcal{U} \mapsto \mathcal{V}$ is defined as

$$\mathcal{G}_N(\mathbf{u}_m)(y) = \sum_{k=1}^p g^N(\mathbf{u}_m; \vartheta^{(k)}) f^N(y; \theta^{(k)}) \quad (12)$$

where \mathcal{U}, \mathcal{V} are function spaces of continuous functions $u \in \mathcal{U}, v \in \mathcal{V}$. \mathbf{u}_m is the evaluation of function u at points $x_i = x_1, \dots, x_m$, p is the number of chosen basis components in the target space, $y \in Y$ is the location of the output function $v(y)$ evaluations, and g^N, f^N are NNs termed branch and trunk

networks. Note, g^N and f^N are not limited to feedforward NNs 10, but can also be of convolutional or recurrent.

Theorem 1: (DeepONet universal approximation theorem [24, Theorem 2.1]). Let $X \subset \mathbb{R}^{d_x}$ and $Y \subset \mathbb{R}^{d_y}$ be compact sets of vectors $x \in X$ and $y \in Y$, respectively. Let $\mathcal{U} : X \rightarrow U \subset \mathbb{R}^{d_u}$ and $\mathcal{V} : Y \rightarrow V \subset \mathbb{R}^{d_v}$ be sets of continuous functions $u(x)$ and $v(y)$, respectively. Let \mathcal{U} be also compact. Assume the operator $\mathcal{G} : \mathcal{U} \rightarrow \mathcal{V}$ is continuous. Then, for all $\epsilon > 0$, there exist $m^*, p^* \in \mathbb{N}$ such that for each $m \geq m^*$, $p \geq p^*$, there exist $\vartheta^{(k)}, \theta^{(k)}$, neural networks $f^N(\cdot; \theta^{(k)}), g^N(\cdot; \vartheta^{(k)})$, $k = 1, \dots, p$, and $x_j \in X, j = 1, \dots, m$, with corresponding $\mathbf{u}_m = (u(x_1), u(x_2), \dots, u(x_m))^T$, such that

$$|\mathcal{G}(u)(y) - \mathcal{G}_N(\mathbf{u}_m)(y)| < \epsilon \quad (13)$$

for all functions $u \in \mathcal{U}$ and all values $y \in Y$ of $\mathcal{G}(u) \in \mathcal{V}$.

Definition 1: (backstepping kernel operator). A mapping $\mathcal{K} : \beta \mapsto k$ of $C^0[0, 1]$ into itself, where $k = \mathcal{K}(\beta)$ satisfies

$$\mathcal{K}(\beta) = -\beta + \beta * \mathcal{K}(\beta), \quad (14)$$

namely, in the Laplace transform notation,

$$k = \mathcal{K}(\beta) := \mathcal{L}^{-1} \left\{ \frac{\mathcal{L}\{\beta\}}{\mathcal{L}\{\beta\} - 1} \right\} \quad (15)$$

is referred to as the *backstepping kernel operator*.

Lemma 1: (Lipschitzness of backstepping kernel operator \mathcal{K}). The kernel operator $\mathcal{K} : \beta \mapsto k$ in Definition 1 is Lipschitz. Specifically, for any $B > 0$ the operator \mathcal{K} satisfies

$$\|\mathcal{K}(\beta_1) - \mathcal{K}(\beta_2)\|_\infty \leq C\|\beta_1 - \beta_2\|_\infty \quad (16)$$

with the Lipschitz constant

$$C = e^{3B} \quad (17)$$

for any pair of functions (β_1, β_2) such that $\|\beta_1\|_\infty, \|\beta_2\|_\infty \leq B$, where $\|\cdot\|_\infty$ is the supremum norm over the argument of β and k .

Proof: Start with the iteration $k^0 = -\beta, k^{n+1} = k^n + \beta * k^n$, $n \geq 0$ and consider the iteration

$$\Delta k^{n+1} = \beta * \Delta k^n, \quad \Delta k^0 = k^0 = -\beta \quad (18)$$

for the difference $\Delta k^n = k^n - k^{n-1}$, which sums to

$$k = \sum_{n=1}^{\infty} \Delta k^n. \quad (19)$$

Next, for $\bar{\beta} = \|\beta\|_\infty$ and all $x \in [0, 1]$,

$$|\Delta k^n(x)| \leq \frac{\bar{\beta}^{n+1} x^n}{n!}, \quad (20)$$

which is established by induction by postulating $|\Delta k^{n-1}(x)| \leq \frac{\bar{\beta}^n x^{n-1}}{(n-1)!}$ and by computing, from (18),

$$\begin{aligned} |\Delta k^n(x)| &= \left| \int_0^x \beta(x-y) \Delta k^{n-1}(y) dy \right| \\ &\leq \bar{\beta} \int_0^x \frac{\bar{\beta}^n y^{n-1}}{(n-1)!} dy \leq \frac{\bar{\beta}^{n+1} x^n}{n!}. \end{aligned} \quad (21)$$

And then, (20) and (19) yield

$$|k(x)| \leq \bar{\beta} e^{\bar{\beta} x}. \quad (22)$$

Next, for $k_1 = \mathcal{K}(\beta_1)$ and $k_2 = \mathcal{K}(\beta_2)$ it is easily verified that

$$k_1 - k_2 = \beta_1 * (k_1 - k_2) - \delta\beta + \delta\beta * k_2 \quad (23)$$

where $\delta\beta = \beta_1 - \beta_2$. Define the iteration

$$\delta k^{n+1} = \beta_1 * \delta k^n \quad (24)$$

$$\delta k^0 = -\delta\beta + \delta\beta * k_2 \quad (25)$$

which verifies $k_1 - k_2 = \sum_{n=1}^{\infty} \delta k^n$. Noting that (22) ensures that $k_2 = \mathcal{K}(\beta_2)$ verifies $|k_2(x)| \leq \bar{\beta}_2 e^{\bar{\beta}_2 x}$, from (25),

$$|\delta k^0(x)| \leq \left(1 + \bar{\beta}_2 e^{\bar{\beta}_2 x}\right) \bar{\delta\beta} \leq \mu_2 \bar{\delta\beta} \quad (26)$$

where $\mu_2 := 1 + \bar{\beta}_2 e^{\bar{\beta}_2}$ and $\bar{\delta\beta} = \|\beta_1 - \beta_2\|_{\infty}$, it can be shown by induction, by mimicking the chain of inequalities (21), that, for all $x \in [0, 1]$,

$$|\delta k^n(x)| \leq \mu_2 \bar{\delta\beta} \frac{\bar{\beta}_1^n x^n}{n!} \quad (27)$$

and therefore it follows that, for all $x \in [0, 1]$,

$$\begin{aligned} |k_1(x) - k_2(x)| &\leq \left(1 + \bar{\beta}_2 e^{\bar{\beta}_2}\right) e^{\bar{\beta}_1 x} \|\beta_1 - \beta_2\|_{\infty} \\ &\leq e^{3B} \|\beta_1 - \beta_2\|_{\infty}. \end{aligned} \quad (28)$$

Hence, local Lipschitzness is proven with (17). ■

Corollary 1: (to Theorem 1). Consider the backstepping kernel operator \mathcal{K} in Definition 1. For all $B > 0$ and $\epsilon > 0$, there exist $p^*(B, \epsilon), m^*(B, \epsilon) \in \mathbb{N}$, with an increasing dependence on B and $1/\epsilon$, such that for each $p \geq p^*$ and $m \geq m^*$ there exist $\theta^{(k)}, \vartheta^{(k)}$, neural networks $f^{\mathcal{N}}(\cdot; \theta^{(k)}), g^{\mathcal{N}}(\cdot; \vartheta^{(k)})$, $k = 1, \dots, p$, and $x_j \in K_1, j = 1, \dots, m$, with corresponding $\beta_m = (\beta(x_1), \beta(x_2), \dots, \beta(x_m))^T$, such that

$$|\mathcal{K}(\beta)(x) - \mathcal{K}_{\mathbb{N}}(\beta_m)(x)| < \epsilon \quad (29)$$

holds for all Lipschitz β with the property that $\|\beta\|_{\infty} \leq B$.

So the backstepping kernel is approximable, qualitatively, but how many neurons and how much data are needed for a given ϵ ? We recall a result on the minimum-sized DeepONet.

Proposition 1: (DeepONet size for kernel operator approximation [24, Theorem 3.3 and Remark 3.4]). If the kernel operator defined in (14) is Lipschitz (or at least Hölder) continuous, a DeepONet that approximates it to a required error tolerance $\epsilon > 0$ indicated by (29) employs the number of data point evaluations for β on the order of

$$m \sim \epsilon^{-1}, \quad (30)$$

the number of basis components in the interpolation when reconstructing into $C^0[0, 1]$ on the order of

$$p \sim \epsilon^{-\frac{1}{2}}, \quad (31)$$

the numbers of layers $L_{g^{\mathcal{N}}}$ in the branch network and of neurons $N_{g^{\mathcal{N}}}$ in each layer of the branch network on the order given, respectively, by

$$N_{g^{\mathcal{N}}} \cdot L_{g^{\mathcal{N}}} \sim \left(\frac{1}{\epsilon}\right)^{\frac{1}{\epsilon}}, \quad (32)$$

and the total size of the trunk network on the order of

$$|\theta^{(k)}| \sim \left(\frac{3}{2} \log \frac{1}{\epsilon}\right)^2. \quad (33)$$

Example 1: In Figure 2 we present two examples of approximation of k using a DeepONet approximation of $\mathcal{K}(\beta)$ for given β_1 and β_2 , which are taken as Chebyshev polynomials $\beta(x) = 6 \cos(\gamma \cos^{-1}(x))$. They are trained on approximating kernels from 900 samples with $\gamma \in \text{uniform}[2, 8]$.

IV. STABILITY UNDER KERNEL APPROXIMATION WITH DEEPONET

For our stability study under an approximate (imperfect) kernel, we begin with a derivation of the target PDE system under a backstepping transformation employing a DeepONet approximation of the backstepping kernel.

For a given β , let $\hat{k} = \hat{\mathcal{K}}(\beta)$, where $\hat{\mathcal{K}} = \mathcal{K}_{\mathbb{N}}$, denote an NO approximation of the exact backstepping kernel k whose existence is established in Corollary 1 for DeepONet. Let

$$\tilde{k} = k - \hat{k} \quad (34)$$

denote the approximation error. Finally, let the backstepping transformation with the approximate kernel \hat{k} be

$$\hat{w} = u - \hat{k} * u. \quad (35)$$

With routine calculations, employing the approximate backstepping transformation and the feedback

$$U = (\hat{k} * u)(1) \quad (36)$$

we arrive at the target system

$$\hat{w}_t = \hat{w}_x + \delta \hat{w}(0) \quad (37)$$

$$\hat{w}(1) = 0, \quad (38)$$

where the function $\delta(x)$ is defined as

$$\delta = -\tilde{k} + \beta * \tilde{k}. \quad (39)$$

Next, we proceed with a Lyapunov analysis.

Lemma 2: (a Lyapunov estimate). Given arbitrarily large $B > 0$, for all Lipschitz β with $\|\beta\|_{\infty} \leq B$, and for all neural operators $\hat{\mathcal{K}}$ with $\epsilon \in (0, \epsilon^*)$, where

$$\epsilon^*(B) = \frac{ce^{-c/2}}{1+B} \quad (40)$$

the Lyapunov functional

$$V(t) = \int_0^1 e^{cx} \hat{w}^2(x, t) dx, \quad c > 0. \quad (41)$$

satisfies the following estimate along the solutions of the target system (37), (38),

$$V(t) \leq V(0)e^{-c^* t}, \quad (42)$$

for

$$c^* = c - \frac{e^c}{c} \epsilon^2 (1+B)^2 > 0. \quad (43)$$

The accuracy required of the NO $\hat{\mathcal{K}}$, and given by (40), is maximized with $c = 2$ and has the value $\epsilon^*(B) = \frac{2}{e(1+B)}$.

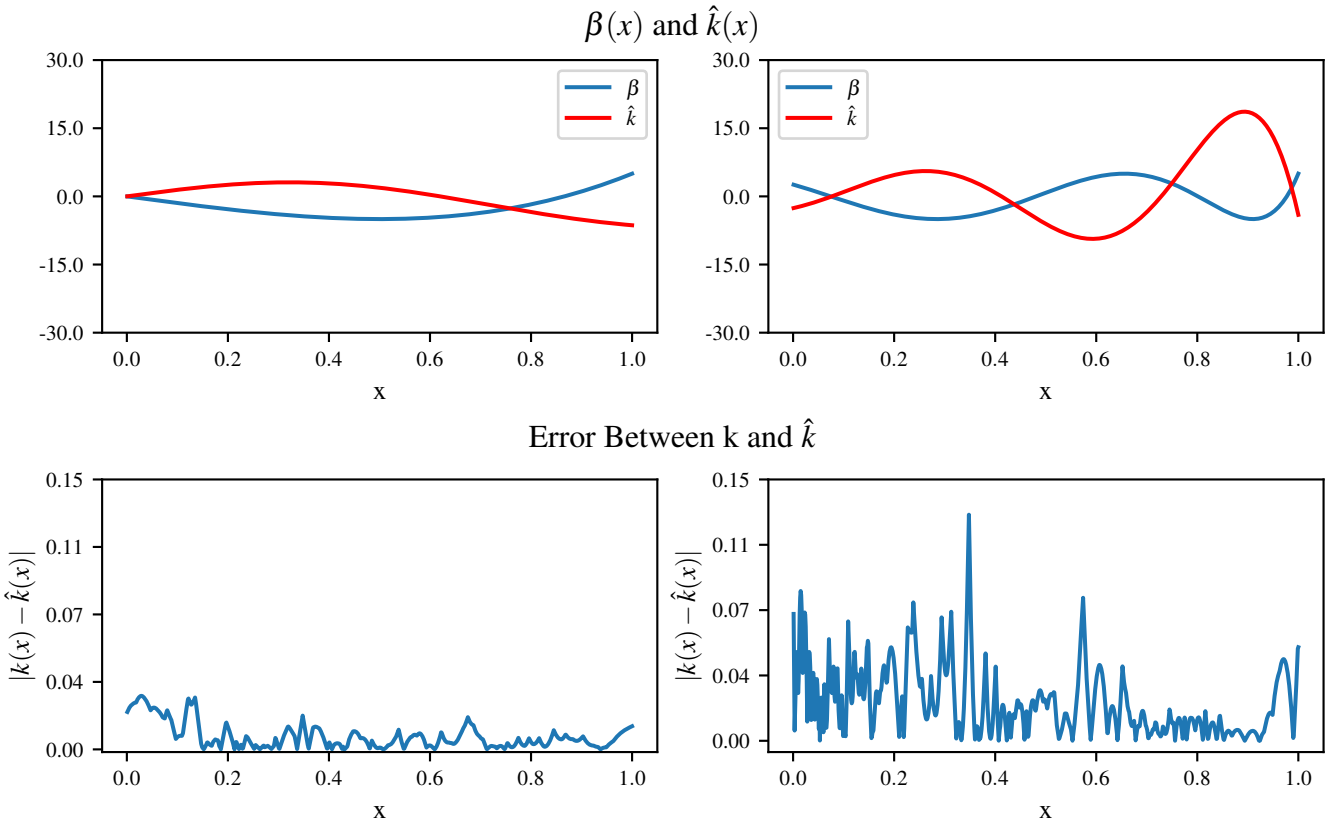


Fig. 2. Examples of β, \hat{k} for Chebyshev polynomials defined as $\beta = 6 \cos(\gamma \cos^{-1}(x))$ with $\gamma = 3, 7.35$ on the left and right respectively. The γ parameter controls the wave frequency of β and therefore affects the resulting kernel. Additionally, the DeepONet absolute approximation error of \hat{k} and k is shown. The DeepONet approximates the "smoother" function on the left with better precision than the large, oscillating function on the right.

Proof: Several steps of calculation (chain rule, substitution, integration by parts) result in

$$\begin{aligned} \dot{V} &= -\hat{w}^2(0) - c \int_0^1 e^{cx} \hat{w}^2(x, t) dx \\ &\quad + \hat{w}(0) \int_0^1 \delta(x) e^{cx} \hat{w}(x) dx \\ &\leq -\frac{1}{2} w^2(0) - c \int_0^1 e^{cx} \hat{w}^2(x, t) dx \\ &\quad + \left(\int_0^1 \delta(x) e^{cx} \hat{w}(x) dx \right)^2 \end{aligned} \quad (44)$$

With the Cauchy-Schwartz inequality

$$\begin{aligned} &\left(\int_0^1 \delta(x) e^{cx} \hat{w}(x) dx \right)^2 \\ &\leq \int_0^1 \delta^2(x) e^{cx} dx \int_0^1 e^{cx} \hat{w}(x)^2 dx \end{aligned} \quad (45)$$

we get

$$\dot{V} \leq -\frac{1}{2} w^2(0) - \left(c - \int_0^1 \delta^2(x) e^{cx} dx \right) V \quad (46)$$

The function δ in (39) is bounded by $|\delta(x)| \leq (1 + \|\beta\|_\infty) \|\tilde{k}\|_\infty$ which, in turn, using (29), yields

$$|\delta(x)| \leq (1 + \bar{\beta})\epsilon =: \bar{\delta}. \quad (47)$$

Then, substituting this into (37), we obtain:

$$\begin{aligned} \dot{V} &\leq -\frac{1}{2} w^2(0) - \left(c - \epsilon^2 (1 + \bar{\beta})^2 \int_0^1 e^{cx} dx \right) V \\ &\leq -\frac{1}{2} w^2(0) - \left(c - \frac{e^c}{c} \epsilon^2 (1 + \bar{\beta})^2 \right) V \\ &\leq -\frac{1}{2} w^2(0) - \left(c - \frac{e^c}{c} \epsilon^2 (1 + B)^2 \right) V \end{aligned} \quad (48)$$

For $0 \leq \epsilon \leq \epsilon^*$, where ϵ^* is defined in (40), we have

$$\dot{V} \leq -\frac{1}{2} w^2(0) - c^* V \quad (49)$$

for some $c^* > 0$ in (43). ■

The size of the NO and of the dataset needs to increase with $\bar{\beta}$, i.e., with the potential instability in the open-loop system.

Lemma 3: (bound on inverse approximate kernel). The kernel \hat{l} of the inverse to the backstepping transformation (35),

$$u = \hat{w} + \hat{l} * \hat{w}, \quad (50)$$

satisfies, for all $x \in [0, 1]$, the estimate

$$|\hat{l}(x)| \leq (\bar{\beta} + (1 + \bar{\beta})\epsilon) e^{(1+\bar{\beta})\epsilon x}. \quad (51)$$

Proof: It is easily shown that \hat{l} obeys the integral equation

$$\hat{l} = -\beta + \delta + \delta * \hat{l}. \quad (52)$$

Using the successive approximation approach, we get that the following bound holds for all $x \in [0, 1]$:

$$|\hat{l}(x)| \leq (\bar{\beta} + \bar{\delta}) e^{\bar{\delta}x}. \quad (53)$$

With (47), we get (51). \blacksquare

Theorem 2: (*Closed-loop stability robust to DeepONet approximation of backstepping kernel*). Let $B > 0$ be arbitrarily large and consider the closed-loop system consisting of (1), (2) with any Lipschitz β such that $\|\beta\|_\infty \leq B$, and the feedback (36) with the NO gain kernel $\hat{k} = \hat{\mathcal{K}}(\beta)$ of arbitrary desired accuracy of approximation $\epsilon \in (0, \epsilon^*)$ in relation to the exact backstepping kernel k , where $\epsilon^*(B)$ is defined in (40). This closed-loop system obeys the exponential stability estimate

$$\|u(t)\| \leq M e^{-c^* t/2} \|u(0)\|, \quad \forall t \geq 0 \quad (54)$$

with the overshoot coefficient

$$M = \left(1 + (\bar{\beta} + (1 + \bar{\beta})\epsilon) e^{(1+\bar{\beta})\epsilon}\right) \left(1 + \bar{\beta} e^{\bar{\beta}}\right) e^{c/2}. \quad (55)$$

Proof: First, we note that V Lemma 2 satisfies

$$\frac{1}{(1 + \|\hat{l}\|_\infty)^2} \|u\|^2 \leq V \leq e^c \left(1 + \|\hat{k}\|_\infty\right)^2 \|u\|^2. \quad (56)$$

Since, by Lemma 2, $V(t) \leq V(0)e^{-c^* t}$, we get, for all $t \geq 0$,

$$\begin{aligned} \|u(t)\| &\leq \left(1 + \|\hat{l}\|_\infty\right) \left(1 + \|\hat{k}\|_\infty\right) e^{c/2} \\ &\times e^{-c^* t/2} \|u(0)\|. \end{aligned} \quad (57)$$

Then, noting, with Theorem 1, (22), and Lemma 3 that

$$\|\hat{k}\|_\infty \leq \|k\|_\infty + \epsilon \leq \bar{\beta} e^{\bar{\beta}} + \epsilon \quad (58)$$

$$\|\hat{l}\|_\infty \leq (\bar{\beta} + (1 + \bar{\beta})\epsilon) e^{(1+\bar{\beta})\epsilon} \quad (59)$$

we finally arrive at the exponential stability estimate (54). \blacksquare

Remark 1: Full-state measurement $u(x, t)$ is employed in the feedback law (36) but can be avoided by employing only the measurement of the outlet signal, $u(0, t)$, from which the full state $u(x, t)$ is observable, the observer

$$\check{u}_t = \check{u}_x + \beta u(0) \quad (60)$$

$$\hat{u}(1) = U \quad (61)$$

and the observer-based controller

$$U = (\hat{k} * \check{u})(1), \quad (62)$$

which can avoid solving the PDE (60), (61) online by employing its explicit solution as an arbitrary function $\check{u}(x, t) = \check{u}_0(x)$ for $t + x \in [0, 1]$ and

$$\check{u}(x, t) = U(t + x - 1) + \int_{t+x-1}^t \beta(t + x - \tau) u(0, \tau) d\tau \quad (63)$$

for $t + x \geq 1$. A closed-loop stability result as in Theorem 2 can be established for this observer-based controller.

V. SIMULATIONS: STABILIZATION WITH NO-APPROXIMATED GAIN KERNEL $\beta \mapsto \mathcal{K}(\beta)$

Continuing with Example 1, in Figure 3 we show that the system is open-loop unstable for both β s and we present tests with the learned kernels in closed-loop simulations up to $t = 2$. In both cases, the PDE settles (nearly perfectly) by $t = 1$, as expected from the target system with the perfect kernel k . The small ripple in the right simulation is due to the use of the approximated kernel \hat{k} . The simulations confirm the theoretical guarantee that an NO-approximated kernel can successfully emulate a backstepping kernel while maintaining stability.

The NO architecture in $\hat{\mathcal{K}}$ consists of about 680 thousand parameters with a training time of 1 minute (using an Nvidia RTX 3090Ti GPU) on a dataset of 900 different β defined as the Chebyshev polynomials $\beta = 6 \cos(\gamma \cos^{-1}(x))$ where $\gamma \sim \text{uniform}(2, 10)$. We choose β of this form due to the rich set of PDEs and kernel functions constructed by varying only a single parameter. The resulting training relative L_2 error $4e-3$ and the testing relative L_2 loss on 100 instances sampled from the same distribution was $5e-3$. If a wider distribution of γ is chosen, the mapping can be learned but requires both a larger network and more data for the same accuracy.

VI. APPROXIMATING THE FULL FEEDBACK LAW MAP $(\beta, u) \mapsto U$

We have so far pursued only the approximation of operator $\mathcal{K}(\beta)$, while treating the feedback operator (8), given by $U = (k * u)(1) = (\mathcal{K}(\beta) * u)(1)$, as straightforward to compute—merely an integral in x , i.e., a simple inner product between the functions $\mathcal{K}(\beta)(1-x)$ and the state measurement $u(x, t)$.

It is of theoretical (if not practical) interest to explore the neural approximation of the mapping from (β, u) into the scalar control input U . Such a mapping is clearly from a much larger space of functions (β, u) into scalars (i.e., the mapping is *functional*) and is, therefore, considerably more training-intensive and learning-intensive. Nevertheless, since it is legitimate to ask how one would approximate not just the feedback gain kernel but the entire feedback law map, we examine this option in this section.

We emphasize that we are approximating just the feedback operator $(\mathcal{K}(\beta) * u)(1)$, whose second argument is the current state u as a function of x , not the entire trajectory $u(x, t)$. We do not train the NO using a trajectory-dependent cost $\int_0^{t_f} \left(\int_0^1 u^2(x, t) dx + U^2(t) \right) dt$ for different initial conditions u_0 , as, e.g., in the application of RL to the hyperbolic PDEs of traffic flow in [86]. Instead, we perform the training simply on the kernel integral equation (14) and the convolution operation (8) for sample functions β and u of x .

The form of stability we achieve in this section is less strong than in Theorem 2. While Theorem 2 guarantees global exponential stability, here we achieve only *semiglobal practical* exponential stability. Because in this section we do not just train a multiplicative gain $\mathcal{K}(\beta)$ but a feedback of u as well, the approximation error is not just multiplicative but additive, which is the cause of the exponential stability being *practical*. Because the data set involves samples u of bounded magnitude, stability is *semiglobal* only.

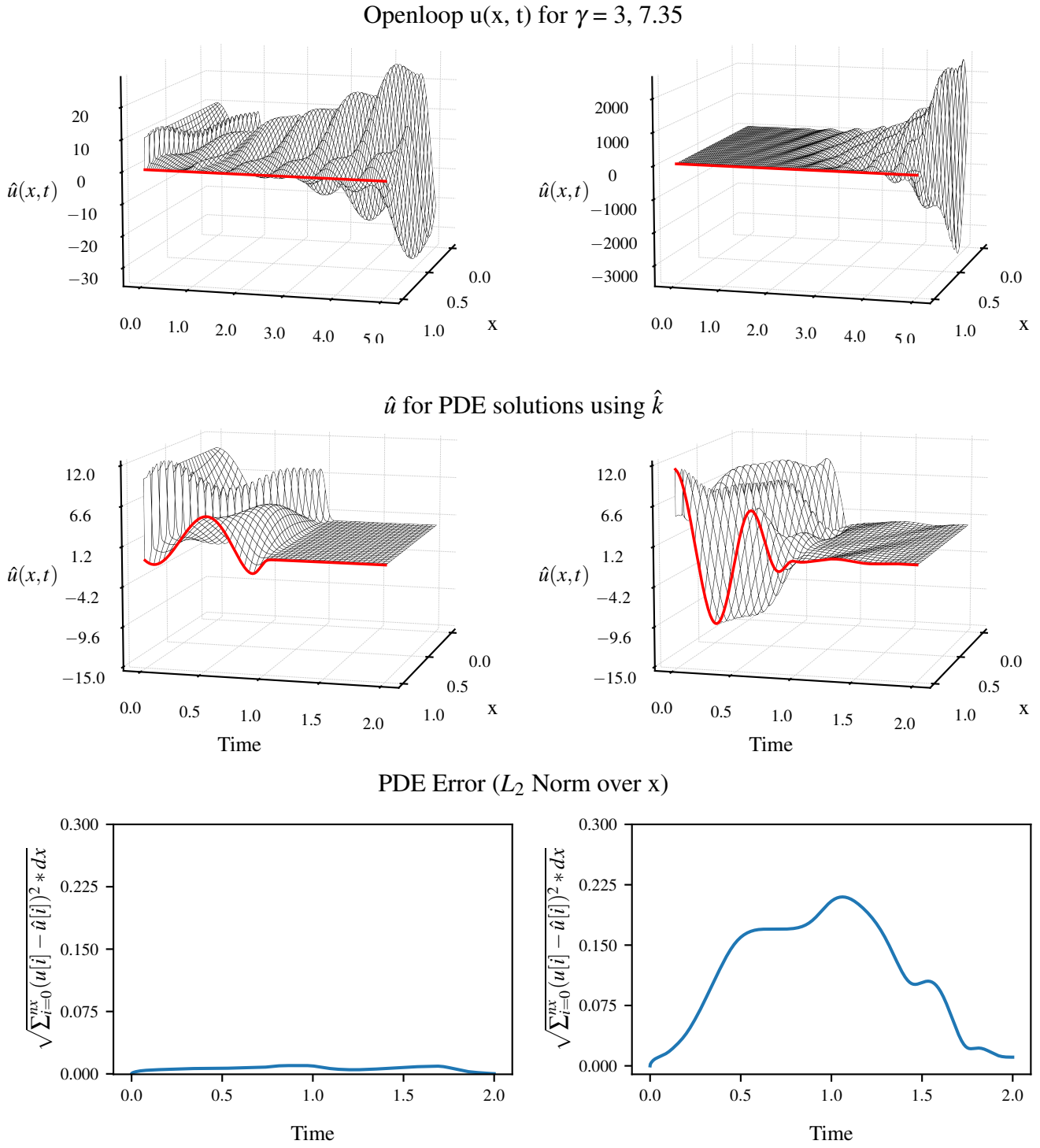


Fig. 3. Top row showcases open-loop instability for the recirculation functions β that are the same as in Fig. 2, with $\gamma = 3, 7.35$ on the left and right respectively. Additionally, the bottom two rows highlight examples of PDE closed-loop state response and errors between the response with “perfect gain” k and “approximate gain” \hat{k} . β corresponds to the same values in Figure 2. For the more “fluctuating” plant parameter β , on the right of Figure 2, the control task is more challenging and, consequently, the state approximation error is also higher (bottom right).

Nevertheless, in comparison to the training on closed-loop solutions over a finite time horizon for the traffic flow in [86], where the finite horizon precludes the possibility of stability guarantees, the semiglobal practical exponential stability achieved here is a rather strong result.

We start by establishing the Lipschitzness of the backstep-

ping feedback map.

Lemma 4: Consider the feedback (8), namely,

$$U = (\mathcal{K}(\beta) * u)(1), \quad (64)$$

and the associated map $\mathcal{U} : (\beta, u) \mapsto U$ from $C^0([0, 1]^2)$ into \mathbb{R} . For arbitrary $B_\beta, B_u > 0$, the mapping \mathcal{U} is Lipschitz on

any set of x -dependent Lipschitz functions (β, u) such that $\|\beta\|_\infty \leq B_\beta$, $\|u\|_\infty \leq B_u$, with a Lipschitz constant

$$\mathcal{U} = B_\beta e^{B_\beta} + B_u e^{3B_\beta}. \quad (65)$$

Proof: Let $U_1 = \mathcal{U}(\beta_1, u_1) = (\mathcal{K}(\beta_1) * u_1)(1)$ and $U_2 = \mathcal{U}(\beta_2, u_2) = (\mathcal{K}(\beta_2) * u_2)(1)$. A calculation gives

$$\begin{aligned} |U_1 - U_2| &= |(\mathcal{K}(\beta_1) * u_1)(1) - (\mathcal{K}(\beta_2) * u_2)(1)| \\ &\leq \|\mathcal{K}(\beta_1)\|_\infty \|u_1 - u_2\|_\infty + \|u_2\|_\infty \|\mathcal{K}(\beta_1) - \mathcal{K}(\beta_2)\|_\infty. \end{aligned} \quad (66)$$

Let $\|\beta_1\|_\infty, \|\beta_2\|_\infty \leq B_\beta$ and $\|u_1\|_\infty, \|u_2\|_\infty \leq B_u$. Recall that $\|\mathcal{K}(\beta)\|_\infty \leq B_\beta e^{B_\beta}$ and $\|\mathcal{K}(\beta_1) - \mathcal{K}(\beta_2)\|_\infty \leq e^{3B_\beta} \|\beta_1 - \beta_2\|_\infty$. Then we get

$$\begin{aligned} |\mathcal{U}(\beta_1, u_1) - \mathcal{U}(\beta_2, u_2)| \\ \leq (B_\beta e^{B_\beta} + B_u e^{3B_\beta}) \|(\beta_1 - \beta_2, u_1 - u_2)\|_\infty. \end{aligned} \quad (67)$$

■

Taking the backstepping transformation $w = u - k*u$, where $k = \mathcal{K}(\beta)$ is the exact backstepping kernel for β , we get

$$w_t = w_x \quad (68)$$

$$w(1) = U - (\mathcal{K}(\beta) * u)(1) \quad (69)$$

Let now $\hat{\mathcal{U}}$ be the NO version of the mapping $\mathcal{U}(\beta, u) = (\mathcal{K}(\beta) * u)(1)$. Taking the NO control $U = \hat{\mathcal{U}}(\beta, u)$, we obtain the boundary condition $w(1) = \hat{\mathcal{U}}(\beta, u) - (\mathcal{K}(\beta) * u)(1)$, namely, the target system

$$w_t = w_x \quad (70)$$

$$w(1) = \hat{\mathcal{U}}(\beta, u) - \mathcal{U}(\beta, u) \quad (71)$$

Due to the Lipschitzness of \mathcal{U} , based on the DeepONet approximation accuracy theorem, we get the following.

Lemma 5: For all $B_\beta, B_u > 0$ and ϵ , there exists an NO $\hat{\mathcal{U}}$ such that

$$|\mathcal{U}(\beta, u) - \hat{\mathcal{U}}(\beta, u)| < \epsilon \quad (72)$$

for all $\beta, u \in C^0[0, 1]$ that are Lipschitz in x and such that $\|\beta\|_\infty \leq B_\beta$, $\|u\|_\infty \leq B_u$.

Next, we state and then prove the main result.

Theorem 3: (Semiglobal practical stability under DeepONet approximation of backstepping feedback law). If $\epsilon < \epsilon^*$, where

$$\epsilon^*(B_\beta, B_u, c) := \frac{\sqrt{c}B_u}{e^{c/2}(1+B_\beta)} > 0, \quad (73)$$

and $\|u(0)\| \leq B_u^0$, where

$$B_u^0(\epsilon, B_\beta, B_u, c) := \frac{1}{1+B_\beta e^{B_\beta}} \left(\frac{B_u}{e^{c/2}(1+B_\beta)} - \frac{\epsilon}{\sqrt{c}} \right) > 0, \quad (74)$$

the closed-loop solutions under the NO approximation of the PDE backstepping feedback law, i.e.,

$$u_t(x, t) = u_x(x, t) + \beta(x)u(0, t) \quad (75)$$

$$u(1, t) = \hat{\mathcal{U}}(\beta, u)(t) \quad (76)$$

satisfy the semiglobal practical exponential stability estimate

$$\begin{aligned} \|u(t)\| &\leq (1+B_\beta)(1+B_\beta e^{B_\beta}) e^{c/2} e^{-ct/2} \|u(0)\| \\ &\quad + (1+B_\beta) \frac{e^{c/2}}{\sqrt{c}} \epsilon, \quad \forall t \geq 0. \end{aligned} \quad (77)$$

The estimate (77) is semiglobal because the radius B_u^0 of the ball of initial conditions in $L^2[0, 1]$ is made arbitrarily large by increasing B_u , and by increasing, in accordance with the increase of B_u , the training set size and the number of NN nodes. Nevertheless, though semiglobal, the attraction radius B_u^0 in (74) is much smaller than the magnitude B_u of the samples of u in the training set.

The residual value,

$$\limsup_{t \rightarrow \infty} \|u(t)\| \leq (1+B_\beta) \frac{e^{c/2}}{\sqrt{c}} \epsilon \quad (78)$$

is made arbitrarily small by decreasing ϵ , and by increasing, in accordance with the decrease of ϵ , the training set size and the number of NN nodes. As the magnitude B_β of the (potentially destabilizing) gain samples β used for training grows, the residual error grows.

Proof: (of Theorem 3) To make the notation concise, denote $\tilde{\mathcal{U}} = \mathcal{U} - \hat{\mathcal{U}}$ and note that this mapping satisfies $|\tilde{\mathcal{U}}(\beta, u)| = |w(1)| \leq \epsilon$ for all $\|\beta\|_\infty \leq B_\beta$, $\|u\|_\infty \leq B_u$. Note also that $\tilde{\mathcal{U}}$ depends on ϵ, B_β, B_u through the number of training data and NO size. Consider now the Lyapunov functional $V(t) = \int_0^1 e^{cx} w^2(x, t) dx$. Its derivative is

$$\begin{aligned} \dot{V} &= e^c w^2(1) - w^2(0) - c \int_0^1 e^{cx} w^2(x, t) dx \\ &\leq -cV + e^c w^2(1) \end{aligned} \quad (79)$$

which yields

$$\begin{aligned} V(t) &\leq V(0)e^{-ct} + \frac{e^c}{c} \sup_{0 \leq \tau \leq t} w^2(1, \tau) \\ &\leq V(0)e^{-ct} + \frac{e^c}{c} \sup_{0 \leq \tau \leq t} (\tilde{\mathcal{U}}(\beta, u)(\tau))^2. \end{aligned} \quad (80)$$

Using the facts that

$$\frac{1}{(1+\|l\|_\infty)^2} \|u\|^2 \leq V \leq e^c (1+\|k\|_\infty)^2 \|u\|^2. \quad (81)$$

and $\|k\|_\infty, \|l\|_\infty \leq B_\beta e^{B_\beta}$, $\|l\|_\infty \leq B_\beta$ we get

$$\begin{aligned} \|u(t)\| &\leq (1+B_\beta)(1+B_\beta e^{B_\beta}) e^{c/2} e^{-ct/2} \|u(0)\| \\ &\quad + (1+B_\beta) \frac{e^{c/2}}{\sqrt{c}} \sup_{0 \leq \tau \leq t} |\tilde{\mathcal{U}}(\beta, u)(\tau)|. \end{aligned} \quad (82)$$

The conclusions of the theorem are directly deduced from this estimate and the bound $|\tilde{\mathcal{U}}| < \epsilon$ in Lemma 5. ■

The NO $\hat{\mathcal{U}} : (\beta, u) \mapsto U$ is complex, and therefore computationally burdensome in real time. Why not instead precompute the neural operator $\hat{\mathcal{K}} : \beta \mapsto \hat{k}$ and also find a DeepONet $\hat{\Omega}$ approximation of the bilinear map $\Omega : (k, u) \mapsto U$, which is simply the convolution $\Omega(k, u)(t) = \int_0^1 k(1-x)u(x, t) dy$, and then compute just $\hat{\Omega}(\hat{k}, u)(t)$ in real time, after computing $\hat{k} = \hat{\mathcal{K}}(\beta)$ offline? This is certainly possible. Why haven't we developed the theory for this approach? Simply because the theory for such a "composition-of-operators" approach, for $\hat{\Omega}(\hat{\mathcal{K}}(\beta), u)$, would be hardly any different, but just notionally more involved, than the theory that we provide here for the one-shot neural operator $\hat{\mathcal{U}}(\beta, u)$.

VII. SIMULATIONS: PRACTICAL STABILIZATION WITH NO-APPROXIMATED FEEDBACK LAW $(\beta, u) \rightarrow U$

Learning the map $(\beta, u) \mapsto U$ is harder than $\beta \mapsto k$ due to the combination of two functions, β , and u . We can learn the mapping using a training set defined by β as in Figure 2 with $\gamma \in \text{uniform}(2, 6)$ and random values of u . We present results with the learned mapping in Figure 4 where the learned control contains significant error. Due to this, we see that the PDE in the right of Figure 4 contains a significant ripple past the time $T = 1$ whereas the analytically controlled PDE is stabilized, as stipulated by the target system, by $T = 1$. When compared to the operator approximation for gain kernel in Figure 3 left, the PDE error is at least twice as large confirming the theoretical results in Theorem 3 and Theorem 2.

Furthermore, the network architecture, as presented in Figure 5 requires significant enhancement over a traditional DeepONet. To learn this mapping, we emulate the operator structure where the map (β, u) requires two DeepONet layers for the integral operators adjointed with linear layers for the multiplicative operation. Additionally, to make the network feasible, we use a smaller spatial resolution than in Section V and a larger dataset. The dataset requires a combination of both β and u and thus consists of 50000 instances. Therefore a network of approximately 415 thousand parameters takes approximately 20 minutes to train. We achieved a training relative L_2 error of $7.2e - 3$ and a testing relative L_2 error of $3.3e - 2$. This demonstrates, to the practical user, that the map (β, u) requires more training data and significant architectural enhancements boosting training time, yet the error in Figure 4 is larger compared to employing the learned map $\beta \mapsto k$.

VIII. EXTENSION TO HYPERBOLIC PIDES

We present the “general case” for a class of hyperbolic partial integro-differential equations (PIDE) of the form

$$\begin{aligned} u_t(x, t) &= u_x(x, t) + g(x)u(0, t) \\ &\quad + \int_0^x f(x, y)u(y, t)dy, \quad x \in [0, 1] \end{aligned} \quad (83)$$

$$u(1, t) = U(t). \quad (84)$$

We have left this generalization for the end of the paper for pedagogical reasons—in order not to overwhelm and daze the reader—since the case where the Volterra operator kernel $f(x, y)$ is a function of two variables complicates the treatment considerably. The backstepping transformation is no longer a convolution with a function of a single variable, the gain mapping is no longer of C^0 functions on $[0, 1]$ but of C^1 functions on the triangle $\{0 \leq y \leq x \leq 1\}$, and the DeepONet theorem requires estimates of the derivatives of the backstepping kernel.

While [6, (11)–(17)] shows that (1), (2) can be transformed into (83), (84), this transformation involves a nonlinear mapping $f \mapsto \beta$, which itself would have to be learned to produce an approximation of the complete kernel mapping $(g, f) \mapsto k$ as a composition of two mappings. This is why the results of the previous sections do not provide a solution to the general case (83), (84), but only a pedagogical introduction, and this is why a generalization in this section is necessary.

To find the mapping from the PIDE coefficients (g, f) to the kernel k of the backstepping controller

$$U(t) = \int_0^1 k(1, y)u(y, t)dy, \quad (85)$$

we take the backstepping transform

$$w(x, t) = u(x, t) - \int_0^x k(x, y)u(y, t)dy, \quad (86)$$

which is not a simple convolution as in (5), with a kernel depending on a single argument, and the same target system as in (6), (7), $w_t = w_x$, $w(1) = 0$, which gives the kernel integral equation derived in [40] as

$$k(x, y) = F_0(x, y) + F(g, f, k)(x, y), \quad (87)$$

where

$$F_0(x, y) := -g(x - y) - \int_0^y f(x - y + \xi, \xi)d\xi \quad (88)$$

$$\begin{aligned} F(g, f, \kappa)(x, y) &:= \int_0^{x-y} g(\xi)\kappa(x - y, \xi)d\xi \\ &\quad + \int_0^y \int_0^{x-y} f(\xi + \eta, \eta)\kappa(x - y + \eta, \xi + \eta)d\xi d\eta. \end{aligned} \quad (89)$$

Denote $\mathcal{T} = \{0 \leq y \leq x \leq 1\}$ as the domain of the functions f and k . Further, denote

$$\bar{g} = \sup_{[0, 1]} |g|, \quad \bar{g}' = \sup_{[0, 1]} |g'| \quad (90)$$

$$\bar{f} = \sup_{\mathcal{T}} |f|, \quad \bar{f}_x = \sup_{\mathcal{T}} |f_x|. \quad (91)$$

It was proven in [40] that

$$|k(x, y)| \leq (\bar{g} + \bar{f}) e^{\bar{g} + \bar{f}} =: \bar{k}(\bar{g}, \bar{f}). \quad (92)$$

For the partial derivatives

$$k_x = F_0^x + F(g, f, k_x) \quad (93)$$

$$k_y = F_0^y - F(g, f, k_x) \quad (94)$$

where

$$F_0^x(x, y) = - \int_0^y f_x(x - y + \xi, \xi)d\xi + \phi_0(x, y) \quad (95)$$

$$\begin{aligned} F_0^y(x, y) &= f_x(x, y) + \int_y^x f(\sigma, y)k(x, \sigma)d\sigma - \phi_0(x, y) \end{aligned} \quad (96)$$

$$\phi_0(x, y) = -g'(x - y) + g(x - y)k(x - y, x - y)$$

$$+ \int_0^y f(x - y + \eta, \eta)k(x - y + \eta, x - y + \eta)d\eta \quad (97)$$

it is proven using the same approach (successive approximation, infinite series, induction) that, on the triangle \mathcal{T} ,

$$|k_x(x, y)| \leq (\bar{f}_x + \bar{\phi}_0) e^{\bar{g} + \bar{f}} =: \bar{k}_x(\bar{g}, \bar{g}', \bar{f}, \bar{f}_x) \quad (98)$$

$$|k_y(x, y)| \leq \bar{f}_x + \bar{f}\bar{k} + \bar{\phi}_0 + (\bar{g} + \bar{f})\bar{k}_x \quad (99)$$

where

$$\bar{\phi}_0(\bar{g}, \bar{g}', \bar{f}) := \bar{g}' + (\bar{g} + \bar{f})\bar{k}. \quad (100)$$

Hence, along with the existence, uniqueness, and continuous differentiability of k [40], we have proven the following.

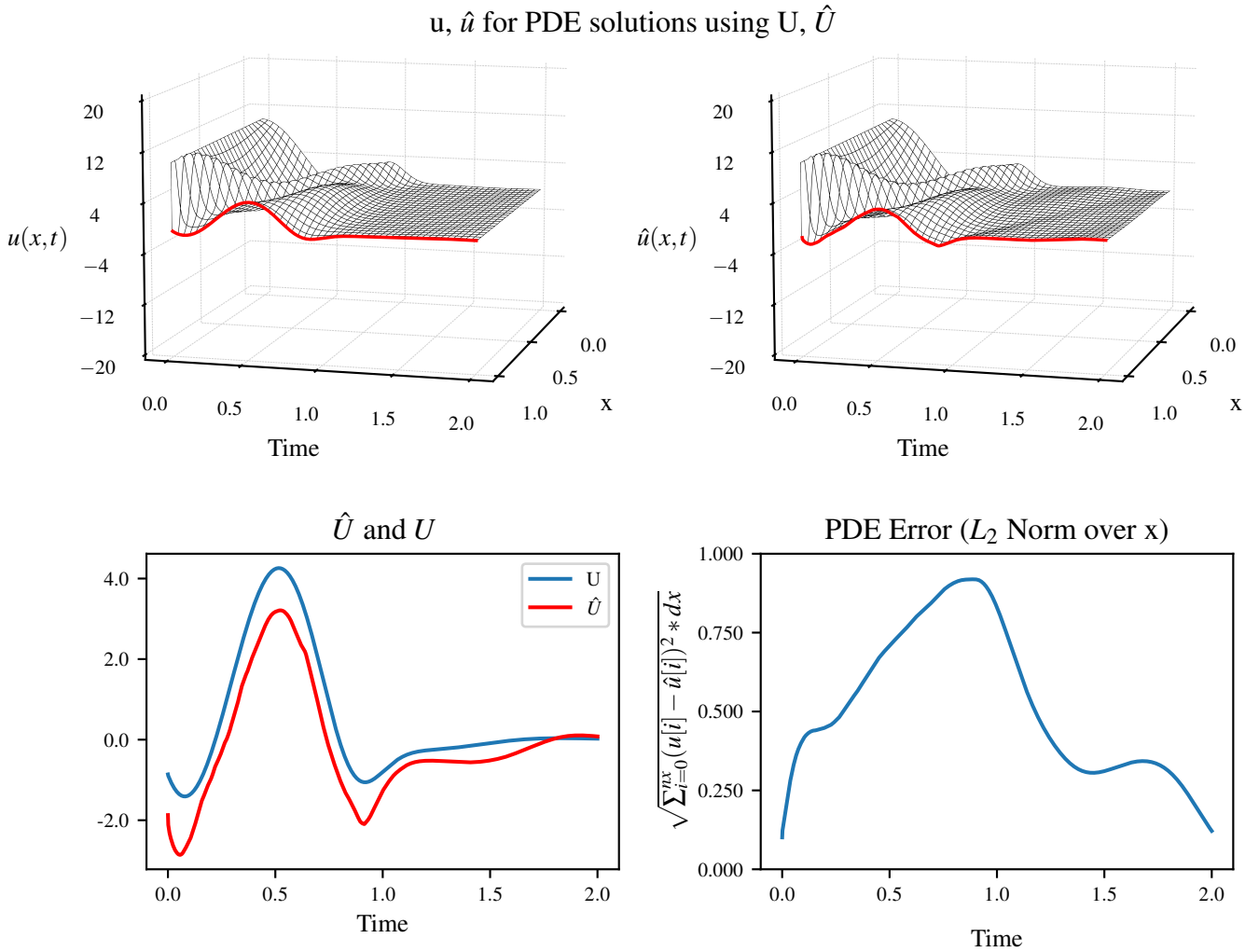


Fig. 4. Examples of PDE closed-loop state response and errors between the response with “perfect control” \mathbf{U} and “approximate control” $\hat{\mathbf{U}}$. β is same as in 2 with $\gamma = 3$.

Lemma 6: The map $\mathcal{Q} : C^1([0, 1] \times \mathcal{T}) \rightarrow C^1([0, 1] \times \mathcal{T})$ defined by $k = \mathcal{Q}(g, f)$, and representing the solution of (87), is continuous. In addition, $|k|, |k_x|, |k_y|$ are bounded, respectively, as in (92), (98), (99), in terms of the bounds on $|g|, |g'|, |f|, |f_x|$.

From the continuity of the map \mathcal{Q} on the Banach space $C^1([0, 1] \times \mathcal{T})$, the following result is inferred from the DeepONet theorem.

Lemma 7: For all $\epsilon > 0$ and $B_g, B_{g'}, B_f, B_{f_x} > 0$ there exists an NO $\hat{\mathcal{Q}}$ such that, for all $(x, y) \in \mathcal{T}$,

$$\begin{aligned} & |\hat{\mathcal{Q}}(g, f)(x, y) - \mathcal{Q}(g, f)(x, y)| \\ & + \left| \frac{\partial}{\partial y} (\hat{\mathcal{Q}}(g, f)(x, y) - \mathcal{Q}(g, f)(x, y)) \right| \\ & + \left| \frac{\partial}{\partial y} (\hat{\mathcal{Q}}(g, f)(x, y) - \mathcal{Q}(g, f)(x, y)) \right| < \epsilon \end{aligned} \quad (101)$$

for all functions $g \in C^1([0, 1])$ and $f \in C^1(\mathcal{T})$ whose derivatives are Lipschitz and which satisfy $\|g\|_\infty \leq B_g$, $\|g'\|_\infty \leq B_{g'}$, $\|f\|_\infty \leq B_f$, $\|f_x\|_\infty \leq B_{f_x}$.

Denoting $\tilde{k} = k - \hat{k} = \mathcal{K}(g, f) - \hat{\mathcal{K}}(g, f)$, (101) can be

written as $|\tilde{k}(x, y)| + |\tilde{k}_x(x, y)| + |\tilde{k}_y(x, y)| < \epsilon$.

Now take the backstepping transformation

$$\hat{w}(x, t) = u(x, t) - \int_0^x \hat{k}(x, y)u(y, t)dy. \quad (102)$$

With the control law

$$U(t) = \int_0^1 \hat{k}(1, y)u(y, t)dy, \quad (103)$$

the target system becomes

$$\begin{aligned} \hat{w}_x(x, t) &= \hat{w}_t(x, t) + \delta(x)\hat{w}(0, t) \\ &+ \int_0^x \delta_1(x, y)u(y, t)dy \end{aligned} \quad (104)$$

$$\hat{w}(1, t) = 0, \quad (105)$$

where

$$\delta_0(x) = -\tilde{k}(x, 0) + \int_0^x g(y)\tilde{k}(x, y)dy \quad (106)$$

$$\begin{aligned} \delta_1(x, y) &= -\tilde{k}_x(x, y) - \tilde{k}_y(x, y) \\ &+ \int_y^x f(\xi, y)\tilde{k}(x, \xi)d\xi \end{aligned} \quad (107)$$

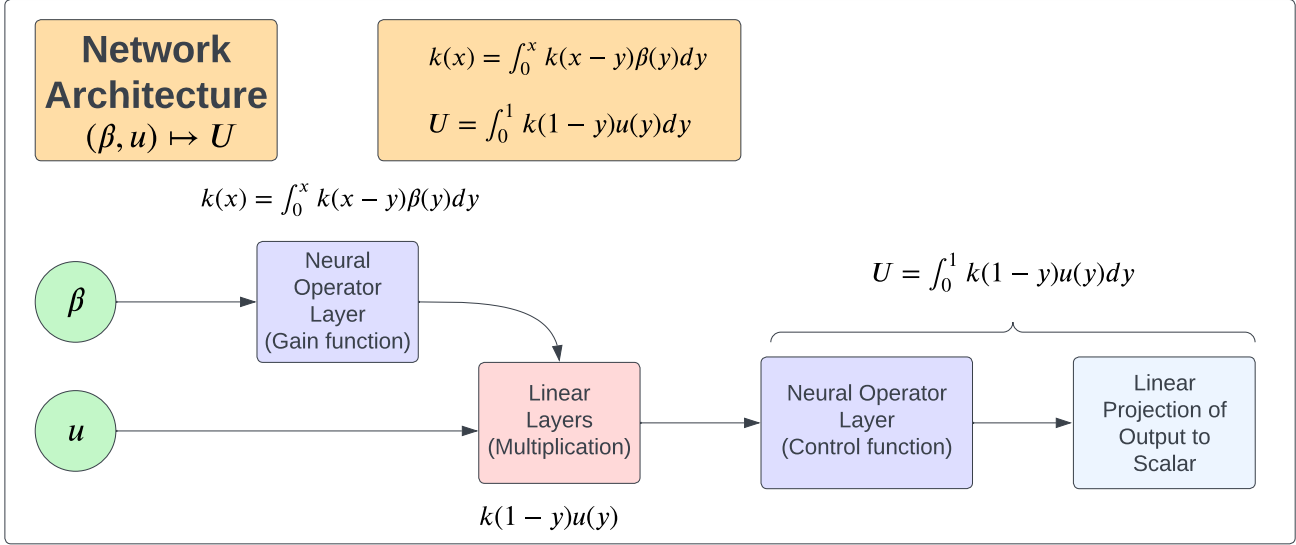


Fig. 5. Network architecture for the map $(\beta, u) \mapsto U$ presented in Section VI. The network first solves the kernel function using a DeepONet layer, then utilizes linear layers to multiply k with the PDE state u , and concludes by learning a second neural operator layer for the nonlinear integral operation yielding the final control output U .

satisfy

$$\|\delta_0\|_\infty \leq (1 + \bar{g})\epsilon \quad (108)$$

$$\|\delta_1\|_\infty \leq (2 + \bar{f})\epsilon. \quad (109)$$

Since the state u appears under the integral in the \hat{w} -system (104), in the Lyapunov analysis we need the inverse backstepping transformation

$$u(x, t) = \hat{w}(x, t) + \int_0^x \hat{l}(x, y)\hat{w}(y, t)dy. \quad (110)$$

It is shown in [41] that the direct and inverse backstepping kernels satisfy in general the relationship

$$\hat{l}(x, y) = \hat{k}(x, y) + \int_y^x \hat{k}(x, \xi)\hat{l}(\xi, y)dy. \quad (111)$$

The inverse kernel satisfies the following conservative bound

$$\|\hat{l}\|_\infty \leq \|\hat{k}\|_\infty e^{\|\hat{k}\|_\infty}. \quad (112)$$

Since $\|\hat{k}\|_\infty < \epsilon$, we have that $\|\hat{k}\|_\infty \leq \|k\|_\infty + \epsilon$. With (92) we get $\|\hat{k}\|_\infty \leq \bar{k}(\bar{g}, \bar{f}) + \epsilon$ and hence

$$\|\hat{l}\|_\infty \leq (\bar{k} + \epsilon) e^{\bar{k} + \epsilon}. \quad (113)$$

Going back to (110), we get

$$\|u\| \leq (1 + (\bar{k} + \epsilon) e^{\bar{k} + \epsilon}) \|\hat{w}\|. \quad (114)$$

Mimicking and generalizing the steps of the proofs of Lemma 2 and Theorem 2, we get the following exponential stability result. (We omit the explicit but conservative and exceedingly complicated and uninformative estimates of the overshoot coefficient, the decay rate, and the upper bound ϵ^* on the approximation accuracy needed to guarantee stability under the gain approximation.)

Theorem 4: Let $B_g, B_{g'}, B_f, B_{f_x} > 0$ be arbitrarily large and consider the system (83), (84) with any $g \in C^1([0, 1])$ and $f \in C^1(\mathcal{T})$ whose derivatives are Lipschitz and which satisfy $\|g\|_\infty \leq B_g$, $\|g'\|_\infty \leq B_{g'}$, $\|f\|_\infty \leq B_f$, $\|f_x\|_\infty \leq B_{f_x}$. There exists a sufficiently small $\epsilon^*(B_g, B_{g'}, B_f, B_{f_x}) > 0$ such that the feedback law (103) with the NO gain kernel $\hat{k} = \hat{\mathcal{Q}}(g, f)$ of arbitrary desired accuracy of approximation $\epsilon \in (0, \epsilon^*)$ in relation to the exact backstepping kernel k ensures that there exist $M, c^* > 0$ such that the closed-loop system satisfies the exponential stability bound

$$\|u(t)\| \leq M e^{-c^* t/2} \|u(0)\|, \quad \forall t \geq 0. \quad (115)$$

IX. SIMULATIONS: STABILIZATION OF PIDE WITH NO-APPROXIMATED GAIN KERNEL $f \mapsto \mathcal{Q}(f)$ DEPENDENT ON (x, y)

For clarity, we consider the systems of the form (83) with $g = 0$, so that the focus is solely on the mapping of two-dimensional plant kernels $f(x, y)$ into two-dimensional backstepping kernels $k(x, y)$, which are governed by the (double) integral equation

$$k(x, y) = - \int_0^y f(x - y + \xi, \xi) d\xi \\ + \int_0^y \int_0^{x-y} f(\xi + \eta, \eta) k(x - y + \eta, \xi + \eta) d\xi d\eta. \quad (116)$$

We illustrate in this section the NO approximation $\hat{\mathcal{Q}}$ of the nonlinear operator $\mathcal{Q} : f \mapsto k$ mapping $C^1(\mathcal{T})$ into itself. First, in Figure 6 we present the construction of the two-dimensional function f via a product of Chebyshev polynomials and highlight the PDE's open-loop instability. Then, we showcase the corresponding learned kernel and the error in Figure 7. The pointwise error for the learned kernel peaks at around 10% of k , as it "ripples" in the right of Figure 7. The

learned kernel \hat{k} achieves stabilization in Figure 8 (right), but not by $t = 1$, as it would with perfect k in (6), (7), but only exponentially, as guaranteed for the learned \hat{k} in Theorem 4.

For this 2D problem (f and k are functions of x and y), we design the branch network of the NO with convolutional neural networks (CNNs) as they have had large success in handling 2D inputs [39], [45]. The network consists of 70 million parameters (due to the CNNs), yet only takes around 5 minutes to train. On 900 instances, the network achieves a relative L_2 training error of $1.3e - 3$ and a relative L_2 testing error of $1.8e - 3$ on 100 instances.

X. CONCLUSIONS

a) What is achieved: PINN, DeepONet, FNO, LOCA, NOMAD—they have all been used with success to approximate solution maps of PDEs. What we introduce is a novel framework: for approximating the solution maps for *integral equations* (87), (88), (89), or simply (9), for the feedback gain functions k in *control of PDEs*.

We provide the guarantees that (i) any desired level of accuracy of NO approximation of the backstepping gain kernel is achieved for any β that satisfies $\|\beta\|_\infty \leq B$ for arbitrarily large given $B > 0$, and (ii) the PDE is stabilized with an NO-approximated gain kernel for any $\|\beta\|_\infty \leq B$.

These results generalize to a class of PIDEs with functional coefficients (g, f) that depends on two variables, (x, y) , and result in kernels k that are also functions of (x, y) .

For a given $B > 0$ and any chosen positive $\epsilon < \epsilon^*(B)$, the determination of the NO approximate operator $\hat{\mathcal{K}}(\cdot)$ is done offline, once only, and such a $\hat{\mathcal{K}}(\cdot)$, which depends on B and ϵ , is usable “forever,” so to speak, for any recirculation kernel that does not violate $\|\beta\|_\infty \leq B$.

When the entire PDE backstepping feedback law—rather than just its gain kernel—is being approximated, globality and perfect convergence are lost, but only slightly. Decay remains exponential, over infinite time, and stability is semiglobal.

b) What is gained by making a particular controller class with theoretical guarantees the object of learning: By now it is probably clear to the reader that what we present here is a method for learning an entire *class* of model-based controllers, by learning the gains $\hat{k} = \hat{\mathcal{K}}(\beta)$, or $\hat{k} = Q(g, f)$, for any plant parameters β or (g, f) . What does one profit from learning a particular class of controllers backed up by theory? Suppose that, instead of learning the *PDE backstepping* gain mapping $\mathcal{K}(\cdot)$, we were trying to find *any* gain function $k(x)$ that meets some performance objective. This goal could be formulated as a finite-time minimization of $\int_0^{t_f} \left(\int_0^1 u^2(x, t) dx + U^2(t) \right) dt$, for a given β , over a set of gain functions k for a ball of initial conditions $u_0(x) = u(x, 0)$ around the origin. Not only would this be a much larger search, over (k, u_0) , but such a finite-time minimization could ensure only finite-time performance, not exponential stability.

Our achievement of global exponential stability (not “practical”/approximate, but with an actual convergence of the state to zero) relies crucially—in each of the lemmas and theorems that we state—on the theoretical steps from the PDE backstepping toolkit (backstepping transform, target system,

integral equation for kernel, successive infinite-series approximation, Lyapunov analysis). It is only by assigning the NO a service role in an otherwise model-based design that stability is assured. Stability assurance is absent from learning approaches in which the feedback law design is left to ML and a finite-time cost, as in RL for the traffic flow PDEs [86].

c) Future research: Of immediate interest are the extensions of the results of this paper to parabolic PDEs in [72], as well as extensions from the approximations of controller kernels to the NO approximations of PDE backstepping observer kernels [73], with guarantees of observer convergence, and with observer-based stabilization (separation principle).

REFERENCES

- [1] H. Anfinsen and O. Aamo. *Adaptive Control of Hyperbolic PDEs*. Springer, 2019.
- [2] A. Aswani, H. Gonzalez, S. S. Sastry, and C. Tomlin. Provably safe and robust learning-based model predictive control. *Automatica*, 49(5):1216–1226, 2013.
- [3] J. Auriol, F. Bribiesca-Argomedo, D. Saba, M. D. Loreto, and F. Di Meglio. Delay-robust stabilization of a hyperbolic PDE-ODE system. *Automatica*, 95:494–502, 2018.
- [4] J. Berberich, C. W. Scherer, and F. Allgöwer. Combining prior knowledge and data for robust controller design. *IEEE Transactions on Automatic Control*, pages 1–16, 2022.
- [5] F. Berkenkamp, M. Turchetta, A. Schoellig, and A. Krause. Safe model-based reinforcement learning with stability guarantees. *Advances in neural information processing systems*, 30, 2017.
- [6] P. Bernard and M. Krstic. Adaptive output-feedback stabilization of non-local hyperbolic PDEs. *Automatica*, 50:2692–2699, 2014.
- [7] D. P. Bertsekas. *Dynamic Programming and Optimal Control*, volume I. Athena Scientific, Belmont, MA, USA, 3rd edition, 2005.
- [8] S. Bhasin, R. Kamalapurkar, M. Johnson, K. Vamvoudakis, F. Lewis, and W. Dixon. A novel actor-critic-identifier architecture for approximate optimal control of uncertain nonlinear systems. *Automatica (Journal of IFAC)*, 49(1):82–92, 2013.
- [9] N. Boffi, S. Tu, N. Matni, J.-J. Slotine, and V. Sindhwan. Learning stability certificates from data. In *Conference on Robot Learning*, pages 1341–1350. PMLR, 2021.
- [10] Y.-C. Chang, N. Roohi, and S. Gao. Neural lyapunov control. *Advances in neural information processing systems*, 32, 2019.
- [11] S. Chen, M. Fazlyab, M. Morari, G. J. Pappas, and V. M. Preciado. Learning lyapunov functions for piecewise affine systems with neural network controllers. *arXiv preprint arXiv:2008.06546*, 2020.
- [12] S. Chen, M. Fazlyab, M. Morari, G. J. Pappas, and V. M. Preciado. Learning lyapunov functions for hybrid systems. In *Proceedings of the 24th International Conference on Hybrid Systems: Computation and Control*, pages 1–11, 2021.
- [13] S. Chen, M. Fazlyab, M. Morari, G. J. Pappas, and V. M. Preciado. Learning region of attraction for nonlinear systems. In *2021 60th IEEE Conference on Decision and Control*, pages 6477–6484. IEEE, 2021.
- [14] S. W. Chen, T. Wang, N. Atanasov, V. Kumar, and M. Morari. Large scale model predictive control with neural networks and primal active sets. *Automatica*, 135:109947, 2022.
- [15] X. Chen and E. Hazan. Black-box control for linear dynamical systems. In *Conference on Learning Theory*, pages 1114–1143. PMLR, 2021.
- [16] J. Choi, F. Castaneda, C. J. Tomlin, and K. Sreenath. Reinforcement learning for safety-critical control under model uncertainty, using control lyapunov functions and control barrier functions. *arXiv preprint arXiv:2004.07584*, 2020.
- [17] Y. Chow, O. Nachum, E. Duenez-Guzman, and M. Ghavamzadeh. A lyapunov-based approach to safe reinforcement learning. *Advances in neural information processing systems*, 2018.
- [18] J. Coron, R. Vazquez, M. Krstic, and G. Bastin. Local exponential H^2 stabilization of a 2×2 quasilinear hyperbolic system using backstepping. *SIAM Journal on Control and Optimization*, 51(3):2005–2035, 2013.
- [19] W. Cui, Y. Jiang, B. Zhang, and Y. Shi. Structured neural-pi control for networked systems: Stability and steady-state optimality guarantees. *arXiv preprint arXiv:2206.00261*, 2022.
- [20] H. Dai, B. Landry, L. Yang, M. Pavone, and R. Tedrake. Lyapunov-stable neural-network control, 2021.

$f(x, y)$ and open loop PDE solution with $f(x, y)$

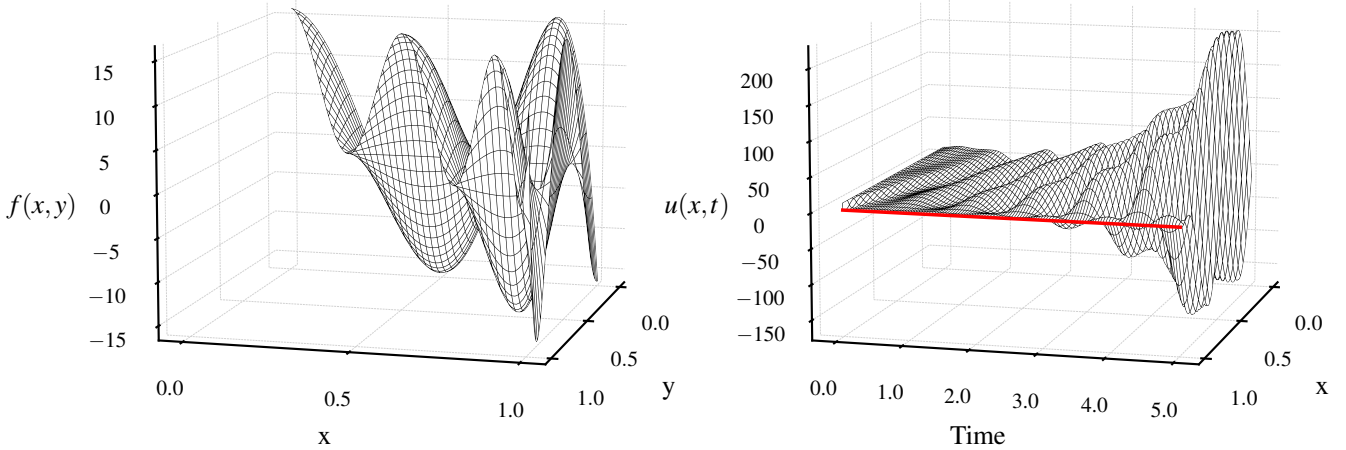


Fig. 6. On the left is an example of $f(x, y)$ generated by the following form $f(x, y) = \beta(x)\beta(y)$ where β is the Chebyshev polynomial as in Fig. 2 with $\gamma = 6$. On the right is the corresponding PDE with open loop instability.

$\hat{k}(x, y)$ and kernel error $k(x, y) - \hat{k}(x, y)$

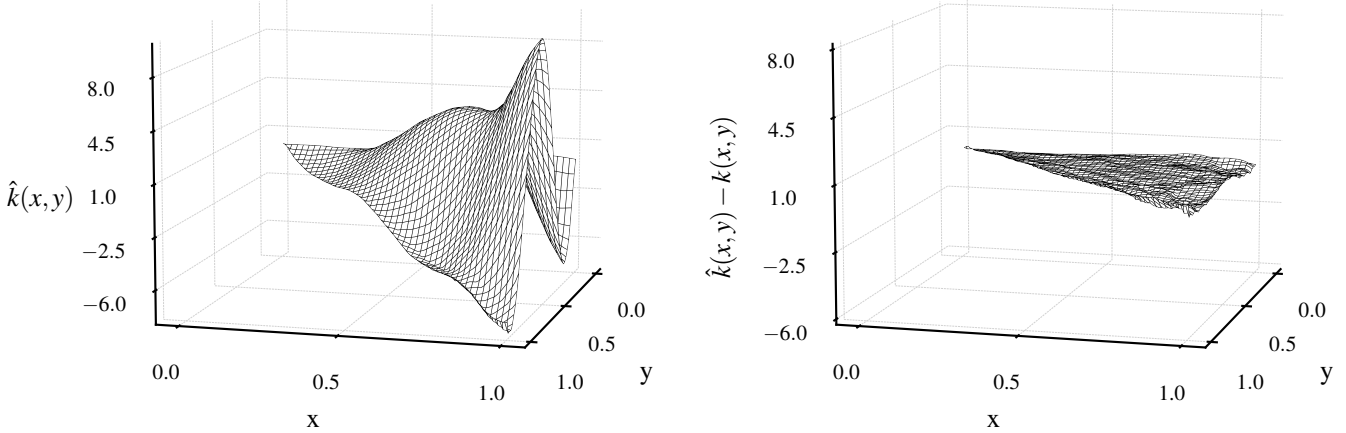


Fig. 7. Examples of the learned kernel $\hat{k}(x, y)$ and the kernel error $k(x, y) - \hat{k}(x, y)$ with a peak of about 10% of $k(x, y)$, around the coordinate $(0.9, 0.9)$. The kernel shown corresponds to $f(x, y)$ in Figure 6.

- [21] C. Dawson, S. Gao, and C. Fan. Safe control with learned certificates: A survey of neural lyapunov, barrier, and contraction methods. *arXiv preprint arXiv:2202.11762*, 2022.
- [22] C. De Persis, M. Rotulo, and P. Tesi. Learning controllers from data via approximate nonlinearity cancellation. *IEEE Transactions on Automatic Control*, pages 1–16, 2023.
- [23] S. Dean, H. Mania, N. Matni, B. Recht, and S. Tu. Regret bounds for robust adaptive control of the linear quadratic regulator. *Advances in Neural Information Processing Systems*, 31, 2018.
- [24] B. Deng, Y. Shin, L. Lu, Z. Zhang, and G. E. Karniadakis. Convergence rate of deeponets for learning operators arising from advection-diffusion equations, 2021.
- [25] J. Deutscher. A backstepping approach to the output regulation of boundary controlled parabolic pdes. *Automatica*, 57:56–64, 2015.
- [26] J. Deutscher and J. Gabriel. Minimum time output regulation for general linear heterodirectional hyperbolic systems. *International Journal of Control*, 93:1826–1838, 2018.
- [27] F. Di Meglio, R. Vazquez, and M. Krstic. Stabilization of a system of $n+1$ coupled first-order hyperbolic linear PDEs with a single boundary input. *IEEE Transactions on Automatic Control*, 58:3097–3111, 2013.
- [28] F. Di Meglio, F. B. Argomedo, L. Hu, and M. Krstic. Stabilization of coupled linear heterodirectional hyperbolic pde–ode systems. *Automatica*, 87:281–289, 2018.
- [29] M. K. S. Faradonbeh, A. Tewari, and G. Michailidis. Finite-time adaptive stabilization of linear systems. *IEEE Transactions on Automatic Control*, 64(8):3498–3505, 2018.
- [30] M. Fazel, R. Ge, S. Kakade, and M. Mesbahi. Global convergence of policy gradient methods for the linear quadratic regulator. In *International conference on machine learning*, pages 1467–1476. PMLR, 2018.
- [31] T. Fiez, B. Chasnov, and L. Ratliff. Implicit learning dynamics in

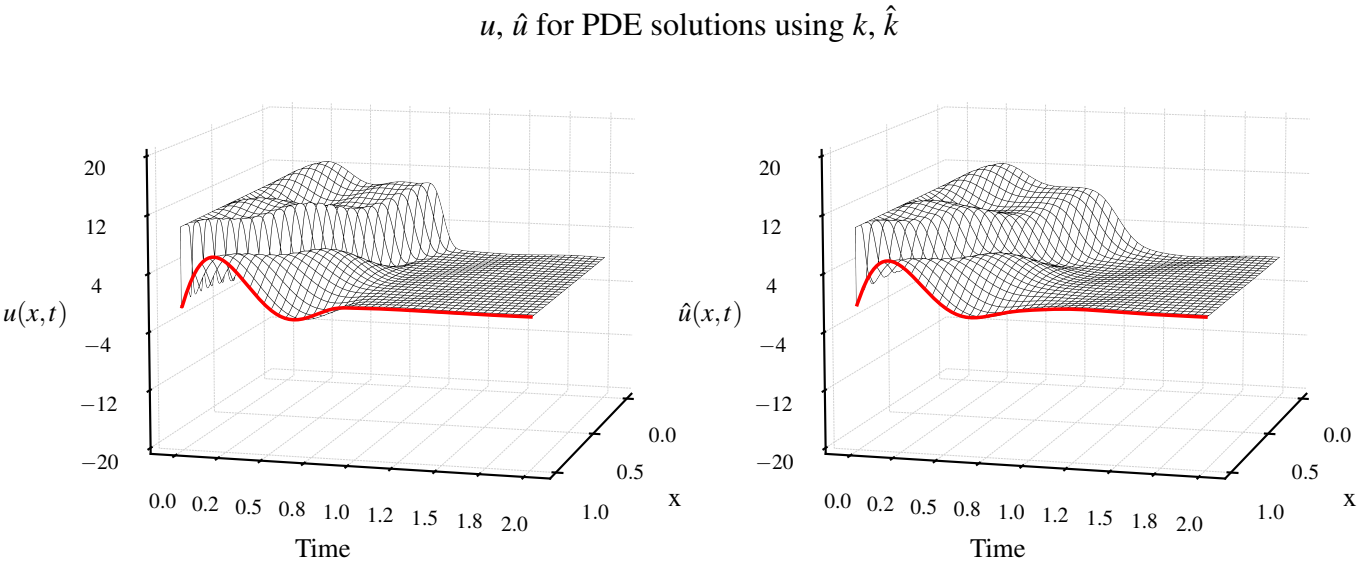


Fig. 8. PDE with the analytical kernel on the top left and with the learned kernel on the top right. Additionally, the L_2 error between the systems peaks around $t = 1.3$ at a value of 0.2. The PDE shown corresponds to the $f(x, y)$ presented in Figure 6.

- stackelberg games: Equilibria characterization, convergence analysis, and empirical study. In *International Conference on Machine Learning*, pages 3133–3144. PMLR, 2020.
- [32] B. Hu, K. Zhang, N. Li, M. Mesbahi, M. Fazel, and T. Başar. Towards a theoretical foundation of policy optimization for learning control policies. *arXiv preprint arXiv:2210.04810*, 2022.
 - [33] L. Hu, F. Di Meglio, R. Vazquez, and M. Krstic. Control of homodirectional and general heterodirectional linear coupled hyperbolic PDEs. *IEEE Transactions on Automatic Control*, 61(11):3301–3314, 2016.
 - [34] L. Hu, R. Vazquez, F. Di Meglio, and M. Krstic. Boundary exponential stabilization of 1-dimensional inhomogeneous quasi-linear hyperbolic systems. *SIAM J. Control and Optimization*, 57(2):963–998, 2019.
 - [35] S. Kakade, A. Krishnamurthy, K. Lowrey, M. Ohnishi, and W. Sun. Information theoretic regret bounds for online nonlinear control. *arXiv preprint*, 2020.
 - [36] G. E. Karniadakis, I. G. Kevrekidis, L. Lu, P. Perdikaris, S. Wang, and L. Yang. Physics-informed machine learning. *Nature Reviews Physics*, 3(6):422–440, 2021.
 - [37] G. Kissas, J. H. Seidman, L. F. Guilhoto, V. M. Preciado, G. J. Pappas, and P. Perdikaris. Learning operators with coupled attention. *Journal of Machine Learning Research*, 23(215):1–63, 2022.
 - [38] N. Kovachki, S. Lanthaler, and S. Mishra. On universal approximation and error bounds for fourier neural operators. *The Journal of Machine Learning Research*, 22(1):13237–13312, 2021.
 - [39] A. Krizhevsky, I. Sutskever, and G. E. Hinton. Imagenet classification with deep convolutional neural networks. In F. Pereira, C. Burges, L. Bottou, and K. Weinberger, editors, *Advances in Neural Information Processing Systems*, volume 25. Curran Associates, Inc., 2012.
 - [40] M. Krstic and A. Smyshlyaev. Backstepping boundary control for first-order hyperbolic PDEs and application to systems with actuator and sensor delays. *Systems & Control Letters*, 57(9):750–758, 2008.
 - [41] M. Krstic and A. Smyshlyaev. *Boundary Control of PDEs: A Course on Backstepping Designs*. SIAM, 2008.
 - [42] S. Lale, K. Azizzadenesheli, B. Hassibi, and A. Anandkumar. Reinforcement learning with fast stabilization in linear dynamical systems. In *International Conference on Artificial Intelligence and Statistics*, pages 5354–5390. PMLR, 2022.
 - [43] S. Lale, Y. Shi, G. Qu, K. Azizzadenesheli, A. Wierman, and A. Anandkumar. Kcrl: Krasovskii-constrained reinforcement learning with guaranteed stability in nonlinear dynamical systems. *arXiv preprint arXiv:2206.01704*, 2022.
 - [44] S. Lanthaler, S. Mishra, and G. E. Karniadakis. Error estimates for DeepONets: a deep learning framework in infinite dimensions. *Transactions of Mathematics and Its Applications*, 6(1), 03 2022. tnac001.
 - [45] Y. LeCun, B. Boser, J. Denker, D. Henderson, R. Howard, W. Hubbard, and L. Jackel. Handwritten digit recognition with a back-propagation network. In D. Touretzky, editor, *Advances in Neural Information Processing Systems*, volume 2. Morgan-Kaufmann, 1989.
 - [46] F. L. Lewis, D. Vrabie, and K. G. Vamvoudakis. Reinforcement learning and feedback control: Using natural decision methods to design optimal adaptive controllers. *IEEE Control Systems Mag.*, 32(6):76–105, 2012.
 - [47] Z. Li, N. Kovachki, K. Azizzadenesheli, B. Liu, K. Bhattacharya, A. Stuart, and A. Anandkumar. Neural operator: Graph kernel network for partial differential equations. *arXiv preprint arXiv:2003.03485*, 2020.
 - [48] Z. Li, N. B. Kovachki, K. Azizzadenesheli, B. Liu, K. Bhattacharya, A. Stuart, and A. Anandkumar. Fourier neural operator for parametric partial differential equations. In *International Conference on Learning Representations*, 2021.
 - [49] Z. Li, M. Liu-Schiavaffini, N. Kovachki, B. Liu, K. Azizzadenesheli, K. Bhattacharya, A. Stuart, and A. Anandkumar. Learning dissipative dynamics in chaotic systems, 2021.
 - [50] Y. Lin, G. Qu, L. Huang, and A. Wierman. Multi-agent reinforcement learning in stochastic networked systems. *Advances in Neural Information Processing Systems*, 34:7825–7837, 2021.
 - [51] L. Lu, P. Jin, and G. E. Karniadakis. Deeponet: Learning nonlinear operators for identifying differential equations based on the universal approximation theorem of operators. *arXiv:1910.03193*, 2019.
 - [52] L. Lu, P. Jin, G. Pang, Z. Zhang, and G. E. Karniadakis. Learning nonlinear operators via deeponet based on the universal approximation theorem of operators. *Nature Machine Intelligence*, 3(3):218–229, 2021.
 - [53] A. A. Malikopoulos. Separation of learning and control for cyber-physical systems. *Automatica*, 151:110912, 2023.
 - [54] W. Mao and T. Başar. Provably efficient reinforcement learning in decentralized general-sum markov games. *Dynamic Games and Applications*, pages 1–22, 2022.
 - [55] E. Mazumdar, L. J. Ratliff, and S. S. Sastry. On gradient-based learning in continuous games. *SIAM Journal on Mathematics of Data Science*, 2(1):103–131, 2020.
 - [56] H. Mohammadi, A. Zare, M. Soltanolkotabi, and M. R. Jovanović. Convergence and sample complexity of gradient methods for the model-free linear–quadratic regulator problem. *IEEE Transactions on Automatic Control*, 67(5):2435–2450, 2021.
 - [57] E. Mojica-Navia, J. I. Poveda, and N. Quijano. Stackelberg population learning dynamics. In *2022 IEEE 61st Conference on Decision and Control (CDC)*, pages 6395–6400. IEEE, 2022.
 - [58] D. Muthirayan, D. Kalathil, and P. P. Khargonekar. Meta-learning online control for linear dynamical systems. In *2022 IEEE 61st Conference on Decision and Control (CDC)*, pages 1435–1440, 2022.

- [59] H. H. Nguyen, T. Zieger, S. C. Wells, A. Nikolakopoulou, R. D. Braatz, and R. Findeisen. Stability certificates for neural network learning-based controllers using robust control theory. In *2021 American Control Conference (ACC)*, pages 3564–3569, 2021.
- [60] B. Pang, T. Bian, and Z.-P. Jiang. Robust policy iteration for continuous-time linear quadratic regulation. *IEEE Transactions on Automatic Control*, 67(1):504–511, 2022.
- [61] B. Pang, Z.-P. Jiang, and I. Mareels. Reinforcement learning for adaptive optimal control of continuous-time linear periodic systems. *Automatica*, 118:109035, 2020.
- [62] D. Pfammatter, T. T. Zhang, S. Tu, and N. Matni. Tasil: Taylor series imitation learning. *arXiv preprint arXiv:2205.14812*, 2022.
- [63] E. Pickering, S. Guth, G. E. Karniadakis, and T. P. Sapsis. Discovering and forecasting extreme events via active learning in neural operators. *Nature Computational Science*, 2(12):823–833, Dec 2022.
- [64] J. I. Poveda, M. Krstic, and T. Basar. Fixed-time nash equilibrium seeking in time-varying networks. *IEEE Transactions on Automatic Control*, 2022.
- [65] G. Qu, A. Wierman, and N. Li. Scalable reinforcement learning of localized policies for multi-agent networked systems. In *Learning for Dynamics and Control*, pages 256–266. PMLR, 2020.
- [66] M. Raissi, P. Perdikaris, and G. E. Karniadakis. Physics-informed neural networks: A deep learning framework for solving forward and inverse problems involving nonlinear partial differential equations. *Journal of Computational physics*, 378:686–707, 2019.
- [67] U. Rosolia and F. Borrelli. Learning model predictive control for iterative tasks: a data-driven control framework. *IEEE Transactions on Automatic Control*, 63(7):1883–1896, 2017.
- [68] J. H. Seidman, G. Kissas, P. Perdikaris, and G. J. Pappas. NOMAD: Nonlinear manifold decoders for operator learning. In A. H. Oh, A. Agarwal, D. Belgrave, and K. Cho, editors, *Advances in Neural Information Processing Systems*, 2022.
- [69] Y. Shi, Z. Li, H. Yu, D. Steeves, A. Anandkumar, and M. Krstic. Machine learning accelerated pde backstepping observers. In *2022 IEEE 61st Conference on Decision and Control (CDC)*, pages 5423–5428, 2022.
- [70] Y. Shi, G. Qu, S. Low, A. Anandkumar, and A. Wierman. Stability constrained reinforcement learning for real-time voltage control. In *2022 American Control Conference (ACC)*, pages 2715–2721. IEEE, 2022.
- [71] S. Singh, S. M. Richards, V. Sindhwani, J.-J. E. Slotine, and M. Pavone. Learning stabilizable nonlinear dynamics with contraction-based regularization. *The International Journal of Robotics Research*, 40(10–11):1123–1150, 2021.
- [72] A. Smyshlyaev and M. Krstic. Closed-form boundary state feedbacks for a class of 1-d partial integro-differential equations. *IEEE Transactions on Automatic Control*, 49(12):2185–2202, 2004.
- [73] A. Smyshlyaev and M. Krstic. Backstepping observers for a class of parabolic pdes. *Systems & Control Letters*, 54(7):613–625, 2005.
- [74] R. S. Sutton and A. G. Barto. *Reinforcement learning: An introduction*. MIT press, 2018.
- [75] Y. Tang, Y. Zheng, and N. Li. Analysis of the optimization landscape of linear quadratic gaussian (lqg) control. In *Learning for Dynamics and Control*, pages 599–610. PMLR, 2021.
- [76] A. J. Taylor, V. D. Dorobantu, M. Krishnamoorthy, H. M. Le, Y. Yue, and A. D. Ames. A control lyapunov perspective on episodic learning via projection to state stability. In *2019 IEEE 58th Conference on Decision and Control (CDC)*, pages 1448–1455. IEEE, 2019.
- [77] A. Tsiamis, I. M. Ziemann, M. Morari, N. Matni, and G. J. Pappas. Learning to control linear systems can be hard. In *Conference on Learning Theory*, pages 3820–3857. PMLR, 2022.
- [78] K. G. Vamvoudakis. Q-learning for continuous-time linear systems: A model-free infinite horizon optimal control approach. *Systems & Control Letters*, 100:14–20, 2017.
- [79] K. G. Vamvoudakis and F. L. Lewis. Online actor-critic algorithm to solve the continuous-time infinite horizon optimal control problem. *Automatica*, 46(5):878–888, 2010.
- [80] K. G. Vamvoudakis, H. Modares, B. Kiumarsi, and F. L. Lewis. Game theory-based control system algorithms with real-time reinforcement learning: How to solve multiplayer games online. *IEEE Control Systems Magazine*, 37(1):33–52, 2017.
- [81] J. Wang and M. Krstic. Delay-compensated control of sandwiched ode-pde-ode hyperbolic systems for oil drilling and disaster relief. *Automatica*, 120:109131, 2020.
- [82] J. Wang and M. Krstic. Event-triggered output-feedback backstepping control of sandwich hyperbolic pde systems. *IEEE Transactions on Automatic Control*, 67(1):220–235, 2022.
- [83] S. Wang, H. Wang, and P. Perdikaris. Learning the solution operator of parametric partial differential equations with physics-informed deep-nets. *Science Advances*, 7(40):eabi8605, 2021.
- [84] H. Yu and M. Krstic. Traffic congestion control for Aw-Rascle-Zhang model. *Automatica*, 100:38–51, 2019.
- [85] H. Yu and M. Krstic. *Traffic Congestion Control by PDE Backstepping*. Springer, 2022.
- [86] H. Yu, S. Park, A. Bayen, S. Moura, and M. Krstic. Reinforcement learning versus pde backstepping and pi control for congested freeway traffic. *IEEE Trans. Control Systems Technology*, 30:1595–1611, 2022.
- [87] K. Zhang, S. Kakade, T. Basar, and L. Yang. Model-based multi-agent rl in zero-sum markov games with near-optimal sample complexity. *Advances in Neural Information Processing Systems*, 33:1166–1178, 2020.
- [88] K. Zhang, Z. Yang, and T. Basar. Policy optimization provably converges to nash equilibria in zero-sum linear quadratic games. *Advances in Neural Information Processing Systems*, 32, 2019.
- [89] K. Zhang, Z. Yang, and T. Başar. Multi-agent reinforcement learning: A selective overview of theories and algorithms. *Handbook of reinforcement learning and control*, pages 321–384, 2021.
- [90] F. Zhao, K. You, and T. Başar. Global convergence of policy gradient primal-dual methods for risk-constrained lqr. *IEEE Transactions on Automatic Control*, 2023.



Luke Bhan received his B.S. and M.S. degrees in Computer Science and Physics from Vanderbilt University in 2022. He is currently pursuing his Ph.D. degree in Electrical and Computer Engineering at the University of California, San Diego. His research interests include neural operators, learning-based control, and control of partial differential equations.



Yuanyuan Shi is an Assistant Professor of Electrical and Computer Engineering at the University of California, San Diego. She received her Ph.D. in Electrical Engineering, masters in Electrical Engineering and Statistics, all from the University of Washington, in 2020. From 2020 to 2021, she was a postdoctoral scholar at the California Institute of Technology. Her research interests include machine learning, dynamical systems, and control, with applications to sustainable power and energy systems.



Miroslav Krstic is Distinguished Professor at UC San Diego, Alspach chair, center director, and Sr. Assoc. Vice Chancellor for Research. He is Fellow of IEEE, IFAC, ASME, SIAM, AAAS, IET (UK), AIAA (Assoc. Fellow), and member of the Serbian Academy of Sciences and Arts, and Academy of Engineering of Serbia. He has received the Richard E. Bellman Control Heritage Award, SIAM Reid Prize, ASME Oldenburger Medal, Nyquist Lecture Prize, Paynter Outstanding Investigator Award, Ragazzini Education Award, IFAC Ruth Curtain Distributed Parameter Systems Award, IFAC Nonlinear Control Systems Award, Chestnut textbook prize, Control Systems Society Distinguished Member Award, the PECASE, NSF Career, and ONR Young Investigator awards, the Schuck ('96 and '19) and Axelby paper prizes. He serves as Editor-in-Chief of Systems & Control Letters, has served as SE in Automatica and IEEE TAC, and is editor of two Springer book series. Krstic has coauthored eighteen books on adaptive, nonlinear, and stochastic control, extremum seeking, control of PDE systems including turbulent flows, and control of delay systems.